KERNFORSCHUNGSANLAGE JÜLICH GmbH

Institut für Plasmaphysik
Association EURATOM-KFA

Hydrodynamic Theory of Convective Transport Across A Dynamically Stabilized Diffuse Boundary Layer

von

H. Gerhauser

Jül - 1869
September 1983
ISSN 0366-0885

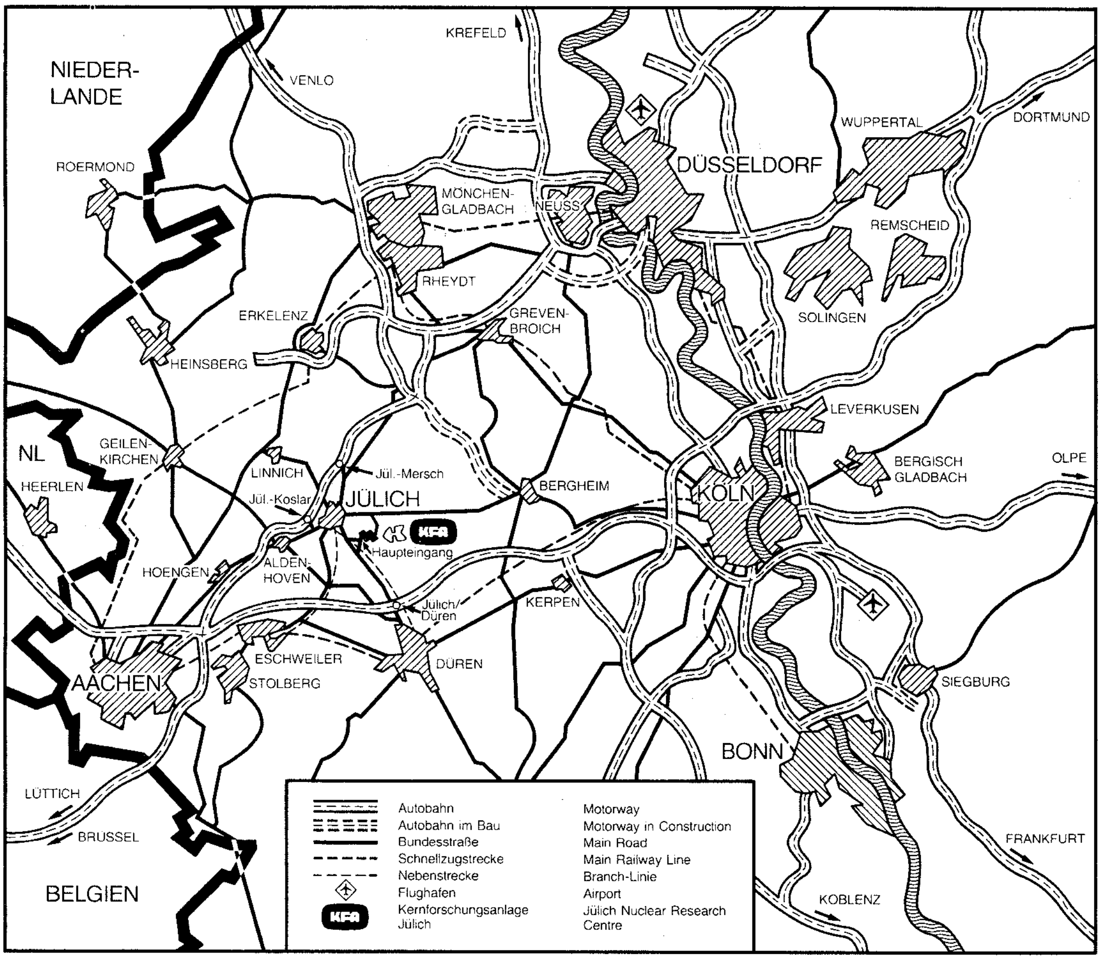

Als Manuskript gedruckt

Berichte der Kernforschungsanlage Jülich – Nr. 1869
Institut für Plasmaphysik, Association EURATOM-KFA, Jül - 1869

Zu beziehen durch: ZENTRALBIBLIOTHEK der Kernforschungsanlage Jülich GmbH
Postfach 1913 · D-5170 Jülich (Bundesrepublik Deutschland)
Telefon: 02461/610 · Telex: 833556-0 kf d

Hydrodynamic Theory of Convective Transport Across A Dynamically Stabilized Diffuse Boundary Layer

von

H. Gerhauser

Hydrodynamic Theory of Convective Transport Across A Dynamically Stabilized Diffuse Boundary Layer

by

Hartmut Gerhauser

Institut für Plasmaphysik der Kernforschungsanlage Jülich GmbH
Association EURATOM-KFA

ABSTRACT

The diffuse boundary layer between miscible liquids is subject to Rayleigh-Taylor instabilities if the heavy fluid is supported by the light one. The resulting rapid interchange of the liquids can be suppressed by enforcing vertical oscillations on the whole system. This dynamic stabilization is incomplete and produces some peculiar novel transport phenomena such as decay of the density profile into several steps, periodic peeling of density sheets off the boundary layer and the appearance of steady vortex flow. The theory presented in this paper identifies the basic mechanism as formation of convective cells leading to enhanced diffusion, and explains previous experimental results with water and ZnJ_2-solutions. A nonlinear treatment of the stationary convective flow problem gives the saturation amplitude of the ground mode and provides an upper bound for the maximum convective transport. The hydrodynamic model can be used for visualizing similar transport processes in the plasma of toroidal confinement devices such as sawtooth oscillations in soft disruptions of tokamak discharges and anomalous diffusion by excitation of convective cells. The latter process is investigated here in some detail, leading to the result that the maximum possible transport is of the order of Bohm diffusion.

CONTENTS

1 INTRODUCTION

Interchange instabilities in superimposed liquids, known as Rayleigh-Taylor instabilities, occur in an inverted density profile, where the density increases in a direction opposite to the gravity force. Such instabilities were first investigated by Lord Rayleigh /1/ in the year 1883.

In the case of a sharp density step at the boundary between non-miscible liquids, perturbations behave as $e^{i(\Omega t - k_x x - k_y y)}$ with

$$\Omega^2 = - gk \frac{\rho_2-\rho_1}{\rho_2+\rho_1} \quad , \quad k = \sqrt{k_x^2 + k_y^2} = k_{||} \tag{1.1}$$

Here ρ_1 is the density of the lower liquid, ρ_2 that of the upper one, the wave vector $\vec{k} = k_x\vec{e}_x + k_y\vec{e}_y$ is parallel to and the gravity acceleration $\vec{g} = - g\,\vec{e}_z$ perpendicular to the boundary layer. Obviously $\rho_2>\rho_1$ leads to instability, and the growth rate $\sigma^2 = -\Omega^2$ tends to infinity with increasing wave number $k = k_{||}$. However, since liquids are always contained in a vessel of finite dimensions, there exists a minimum wave number k_{min} and thus a minimum growth rate $\sigma^2_{min} = - \Omega^2(k_{min})$.

The situation is different in the case of a diffuse boundary layer with a finite density gradient $\nabla\rho = \rho'\vec{e}_z$, as present in the interface of superimposed miscible liquids. In this case there exists an upper limit for the growth rate determined by the thickness h of the boundary layer. For $k_{||}h \to \infty$ we get

$$\sigma^2 \to \sigma^2_{max} = g\,\frac{\rho'}{\rho} \approx g\,\frac{2}{h}\,\frac{\rho_2-\rho_1}{\rho_2+\rho_1} \tag{1.2}$$

where it is supposed that the density difference $\rho_2-\rho_1$ is small compared to the density ρ_1. On the other hand, a diffuse boundary layer allows the formation of modes with a vertical wave number $k_z = k_\perp$, and these modes grow arbitrarily slowly for $k_\perp h \to \infty$. Therefore the growth rates are bounded from above, but not from below.

When applying dynamic stabilization to such a system, the liquid is forced to oscillate with a certain frequency ω perpendicular to the interface. This stabilizes all modes with growth rates σ in a certain interval $\sigma_1<\sigma<\sigma_2$. Modes with $\sigma>\sigma_2$ are not stabilized, they become even destabilized by the excitation of so-called parametric resonances. Thus, for a given set of oscillation parameters, the excitation of the fast growing modes with short wave lengths $\lambda_{||} = 2\pi/k_{||}$ causes, via turbulence, an initially rather sharp interface to get smoothed out and intermixed, until the boundary layer becomes diffuse and finally reaches a thickness h, at which the maximum growth rate is $\sigma_{max}<\sigma_2$. Then the parametric resonances have destroyed their own existence condition. However, the slowly growing modes with short wave lengths $\lambda_\perp = 2\pi/k_\perp$ and $0<\sigma<\sigma_1$ prefer this state of the boundary layer and remain unstabilized, though with reduced growth rates. These modes do not cause a complete interchange of the liquid but produce some peculiar transport phenomena that lead to considerably enhanced diffusion as compared to ordinary diffusion. This "anomalous" transport was first observed and analyzed experimentally by Wolf /2/ and recently investigated in some more detail by Hopmann et al. /3/.

The present paper identifies the basic mechanism of transport through the boundary layer as formation of convective cells, i.e. linked whirls or vortices with mass density roll motion. These convective cells lead to the separation of the boundary layer into several distinct density steps, to intermittent detachment of density sheets off the boundary layers as well as to quasistationary eddy motion. A theoretical analysis of these effects is presented, starting from the theories of Rayleigh /1/ and Wesson /4/. With the aid of Mathieu's stability diagram /5, 6/, the growth-rates of the different modes are calculated and the structure of the fastest or ground mode is analyzed. The motion is continued and considered also in the nonlinear regime where the amplitude of the ground mode saturates. The nonlinear treatment of steady convective eddy flow provides an upper bound for the maximum diffusion coefficient induced by convective transport. The convective motion of the ground mode, by peeling part of the diffuse boundary layer off the interface region, tends to steepen the density profile beyond the threshold for the excitation of the parametric resonances. The latter counteract automatically and start to broaden the density profile below the threshold. The described competitive actions of parametric resonances and convective cell motion establish some sort of dynamic equilibrium maintaining a constant density gradient.

It is pointed out that these nonlinear processes characterizing the transport in the hydrodynamic model reveal some similarity to those found in the magnetized plasma of fusion devices. For example, the periodically intermittent detachment of density sheets off the diffuse boundary layer resembles the periodically repeated expulsion of the hot plasma core in the sawtooth oscillations of tokamaks. In either case the transport is characterized by a sequence of long quiet phases of recovery and growth, alternating with sudden disruptions. This analogy has already been worked out in /7/. Here we concentrate on another phenomenon with an even closer relationship to the hydrodynamic model, the interchange modes, which are excited by a fictitious gravity acceleration (e.g. by field line curvature) and which are partially stabilized by the effect of gyroviscosity, the ion gyro frequency taking the role of the enforced oscillation frequency. The Rayleigh-Taylor unstable interchange modes, localized in the neighbourhood of singular surfaces (flute modes) and in regions of unfavourable curvature (ballooning modes), give rise to convective cells in the plasma which may contribute essentially to the anomalous transport, one of the major problems on the way to controlled nuclear fusion. Starting from a twodimensional two-fluid model and with a proper scaling based on the well-known finite Larmor-radius ordering, the nonlinear theory of the hydrodynamic model can be transferred and applied to the plasma, leading to a system of equations for the description of the nonlinear saturation of the most unstable mode which is essentially identical to the one which holds for the liquid boundary layer. The treatment is even facilitated because there is no need to use Mathieu's functions. The role of the parametric resonances is taken in the plasma by the microturbulence induced by unstable drift waves. In a stationary state of interactive coupling of convective and turbulent transport the maximum possible transport comes out to be of the order of Bohm diffusion.

2 Experimental Observations

The first applications of dynamic stabilization to Rayleigh-Taylor instabilities by Wolf /18/ were restricted to the case of sharp boundary layers. However, in /2/ the same author also carefully investigated the specific phenomena observed in the case of diffuse boundary layers. In the following, his principal experimental data, observations and results are briefly summarized. Water with $\rho_1 = 1\ g/cm^3$ and aqueous solution of zinc iodide with $\rho_2 = 1.8\ g/cm^3$ served as miscible liquids. In addition, experiments were performed in which both the water and the ZnJ_2-solution were mixed with glycerine, so that the viscosity of both liquids was 50 times greater than that of water. The cylindrical glass vessel had a length of $\Lambda = 6$ cm and a diameter of $D = 0.78$ cm. Initially ($t<0$) the lower half was filled with the heavy ZnJ_2-solution, the upper one with water. The diffuse boundary layer remained then in a stable equilibrium. The vessel was shaken parallel to its axis (perpendicular to the boundary layer) with a frequency typically $\nu = 100$ Hz or $\omega = 2\pi\nu = 2\pi\cdot 10^2\ sec^{-1}$. The amplitude of the shaking acceleration was $b_o = 60$ g. At $t = 0$ the vibrating vessel was inverted, so that the heavier fluid was now upside. For $t>0$ the time development of the density profile was observed by photometric light absorption measurements utilizing the yellow colour of ZnJ_2. A striking feature was the decay of the initially continuous density profile into four density steps of about equal height. Instead of one boundary layer with a density difference of $\rho_2-\rho_1 = 0.8\ g/cm^3$ there appeared four successive boundary layers, each with a density difference of about $0.2\ g/cm^3$. The lowest step was not fully developed and disappeared after one minute. The uppermost step broke down after about 6 minutes. After 8 minutes still two steps were left. The further evolution could not be followed since the vibrator switched off due to overheating.

In fig. 1 the experimental density profiles are plotted. The dynamic stabilization maintained a quasistationary grossly stable diffusion equilibrium characterized by the following peculiar phenomena. In almost regular intervals thin sheets of relatively high and of relatively low density were peeled off the diffuse boundary layers, the former sinking down and the latter rising up. By the darker brownish colour of the denser liquid sheets this effect was clearly observable even by visual inspection.

As a consequence of the described nonlinear transport phenomena the density difference at the boundary layers decreased gradually with time until, when $\Delta\rho \lesssim 0.13$ g/cm^3, the density step was liable to sudden breakdown. Of course, the duration until a complete decay of the total density profile is proportional to the length Λ of the vessel. It is about two to three orders of magnitude shorter than the time for density equalization by normal diffusion. Thus the unstabilized modes with short vertical wave lengths caused some kind of anomalously enhanced diffusion. These results were not essentially altered when glycerine was added to increase the viscosity, i.e. even large viscosity could not achieve complete stabilization.

In recent experiments of Hopmann et al. /3/ similar values of the shake-frequency and the acceleration amplitude were applied, but vessels with rectangular cross section were used for improved optical observation. The broad side of the rectangle could be varied and was always much longer than the narrow side, so the wave length of the ground mode which is twice the broad side of the rectangle could be varied as well. It was found that a reduction of the vessel cross section increased the number of density steps and reduced the velocity of diffusive transport. In the case of intermittent detachment of density sheets off the boundary layer their origin sometimes shifted from the right side to the left side of the vessel and vice versa. However, special experimental conditions were found which allowed the formation of stationary vortex motion with a coupled pair of eddies leading to continuous mass transport across the boundary layer. In this case the orientation of the vortices remained constant. Addition of glycerine slowed down the whole process considerably, thus facilitating the observation by film or video camera or by eye. The qualitative character of the described processes was not altered by viscous damping. Future experiments are intended to investigate these effects in a more systematic and quantitative manner.

3 Linear Theory

3.1 Rayleigh-Taylor Instabilities in Diffuse Boundary Layers

Lord Rayleigh /1/, about hundred years ago, was the first to investigate the equilibrium of an incompressible heavy fluid with variable density. In the following his principal assumptions and results are reconsidered, for our purposes in modernized notation and in modified form and with useful extensions. The basic equations are in linearized form

eq. of motion: $$\rho \frac{\partial}{\partial t}\delta\vec{v} = - \nabla\delta p - \delta\rho\cdot g\vec{e}_z \tag{3.1}$$

eq. of continuity: $$\frac{\partial}{\partial t}\, \delta\rho + \rho'\delta v_z = 0 \tag{3.2}$$

eq. of incompressibility: $$\nabla\cdot\delta\vec{v} = 0 \tag{3.3}$$

The density profile is $\rho(z)$, and the density gradient is $\rho' = d\rho/dz$. Perturbed quantities are denoted by δ and assumed to propagate along the x-direction as $e^{i(\Omega t-kx)}$, so that the following differential equation is obtained

$$\left[\frac{d}{dz}\left(\rho\,\frac{d}{dz}\right) - k^2\left(\frac{g\,\rho'}{\Omega^2} + \rho\right)\right]\delta v_z = 0 \tag{3.4}$$

or equivalently

$$\left[\frac{d^2}{dz^2} - k^2 + \frac{\rho'}{\rho}\left(\frac{d}{dz} - \frac{gk^2}{\Omega^2}\right)\right]\delta v_z = 0 \tag{3.5}$$

In the case of a sharp interface at $z = 0$, ρ' vanishes everywhere outside, and it follows

$$\delta v_z = \delta v_z(0)\, e^{\mp kz} \quad \text{for} \quad z \gtrless 0 \tag{3.6}$$

Therefore perturbations with short wave lengths are confined to the immediate neighbourhood of the interface. The derivative $\delta v_z' = d/dz\, \delta v_z$ is discontinuous at the interface. Integration

$\int_{-0}^{+0} \ldots dz$ of (3.4) across the interface yields

$$\left[\rho\delta v_z'\right]_2 - \left[\rho\delta v_z'\right]_1 - \frac{gk^2}{\Omega^2}(\rho_2-\rho_1)\ \delta v_z(0) = 0$$

resulting in the initially cited formula (1.1) for Ω^2. In the case of a diffuse boundary layer, analytic formulas can be obtained only for an exponential density increase, that is

$$\rho(z) = \rho_1\ e^{\beta z},\ \frac{\rho'}{\rho} = \beta \quad \text{for} \quad 0 \le z \le h$$

$$\rho_2 = \rho_1\ e^{\beta h} \tag{3.7}$$

This leads to a differential equation with constant coefficients:

$$\delta v_z'' + \beta\delta v_z' - k^2\ (1 + \frac{g\beta}{\Omega^2})\ \delta v_z = 0 \tag{3.8}$$

The solutions are all of the form $e^{\alpha z}$, and the complex α are the roots of the characteristic equation

$$\alpha^2 + \beta\alpha - k^2\ (1 + \frac{g\beta}{\Omega^2}) = 0. \tag{3.9}$$

The solutions and the growth rates are greatly affected by the boundary conditions. We consider two cases.

3.1.1 Boundary Layer between Solid Walls

If the layer is bounded from below and above by solid walls, the boundary conditions are

$$\delta v_z(0) = \delta v_z(h) = 0 \tag{3.10}$$

and the proper solution is

$$\delta v_z = \delta V\ e^{-\beta z/2}\ \sin\frac{n\pi z}{h}, \quad n = 1, 2, 3, \ldots \tag{3.11}$$

n is the vertical mode number. We obtain Ω by inserting the derivatives into the differential equation:

$$\delta v_z' = \left(-\frac{1}{2}\,\beta + \frac{n\pi}{h}\cot\frac{n\pi z}{h}\right)\delta v_z$$

$$\delta v_z'' = \left(-\frac{1}{2}\,\beta + \frac{n\pi}{h}\cot\frac{n\pi z}{h}\right)\delta v_z' - \frac{(n\pi/h)^2}{\sin^2 n\pi z/h}\,\delta v_z$$

$$\delta v_z''+\beta\delta v_z' = \left(\ \frac{1}{2}\,\beta + \frac{n\pi}{h}\cot\frac{n\pi z}{h}\right)\delta v_z' - \frac{(n\pi/h)^2}{\sin^2 n\pi z/h}\,\delta v_z$$

$$= \left[-\frac{1}{4}\,\beta^2 + \left(\frac{n\pi}{h}\right)^2\cot^2\frac{n\pi z}{h} - \frac{(n\pi/h)^2}{\sin^2 n\pi z/h}\right]\delta v_z$$

$$= -\left[\frac{1}{4}\,\beta^2 + \frac{n^2\pi^2}{h^2}\right]\delta v_z = k^2\left(1 + \frac{g\beta}{\Omega^2}\right)\delta v_z$$

Consequently

$$\frac{g\beta}{\Omega^2} = -\beta 1 = -\frac{\beta^2h^2/4+n^2\pi^2+k^2h^2}{k^2h^2} \tag{3.12}$$

Thus the dispersion relation is found to be

$$\sigma^2 = -\Omega^2 = \frac{g}{1} \quad \text{with} \quad 1 = \frac{\beta^2h^2/4+n^2\pi^2+k^2h^2}{\beta k^2h^2} \tag{3.13}$$

1 is the length of an equivalent pendulum with the same oscillation frequency Ω resp. growth rate σ. Modes with small n and large k have the highest growth rates, and in accordance with (1.2)

$$\sigma^2_{max} = \lim_{k\to\infty}\frac{g}{1} = g\beta = \frac{g\rho'}{\rho} \tag{3.14}$$

Modes with small k and large n, on the other hand, have arbitrarily small growth rates. For moderate density steps $\Delta\rho = \rho_2 - \rho_1$, the term

$$\frac{1}{4}\,\beta^2h^2 \approx \frac{1}{4}\left(\frac{\Delta\rho}{\rho}\right)^2 \le \frac{1}{4} \tag{3.15}$$

may always be neglected against $n^2\pi^2$. The wave number k has only discrete values,

$$k = \frac{2\,\pi}{\lambda} = \frac{2m\pi}{\lambda_{max}} = \frac{m\pi}{D} \tag{3.16}$$

This holds rigorously only for vessels with rectangular cross section, but for $m \ge 2$ it is approximately valid also for vessels with circular cross section. The ground mode in a cylindrical vessel of diameter D, corresponding to m = 1, is given by $k_{min} = \frac{3.68}{D}$, where $J_1'(k_{min}\,D/2) = J_1'(1.84) = 0$. n and m are the numbers of the horizontal and vertical nodal planes of the velocity field, and thus determine the subdivision of the boundary layer into a system of convective cells. For n = 2 and m = 3 we get the convection pattern of fig. 2. The rotation velocity of the convective cells grows $\sim e^{\sigma t}$, the orientation of the linked eddies depends on the accidental initial conditions.

3.1.2 Boundary Layer between Homogeneous Fluids

Let

$$\rho = \rho_1 \quad \text{and} \quad \delta v_z \sim e^{kz} \qquad \text{for } z \leq 0$$

$$\rho = \rho_1 \, e^{\beta z} \qquad \text{for } 0 \leq z \leq h$$

$$\rho = \rho_2 = \rho_1 \, e^{\beta h} \quad \text{and } \delta v_z \sim e^{-kz} \qquad \text{for } z \geq h \tag{3.17}$$

The boundary conditions for continuous transition at the interfaces between the boundary layer and the regions of homogeneous density are

$$\left.\frac{\delta v_z'}{\delta v_z}\right|_0 = k \;, \quad \left.\frac{\delta v_z'}{\delta v_z}\right|_h = -k \tag{3.18}$$

Only this case is of practical interest, since we want to consider a real boundary layer between two different fluids. We assume the z-dependence of the eigenfunction to be

$$\delta v_z = \delta V \; e^{-\frac{1}{2}\beta z} \sin\left(\frac{\phi z}{h} - \varepsilon\right) \quad \text{for } 0 \leq z \leq h \tag{3.19}$$

and obtain in analogy to (3.13) the following equivalent pendulum length

$$l = \frac{\beta^2 h^2/4 + \phi^2 + k^2 h^2}{\beta k^2 h^2} \tag{3.20}$$

For calculating ϕ we need

$$\frac{\delta v_z'}{\delta v_z} = -\frac{1}{2}\beta + \frac{\phi}{h}\cot\left(\frac{\phi z}{h} - \varepsilon\right) \tag{3.21}$$

The boundary conditions yield

$$- \frac{1}{2} \beta - \frac{\phi}{h} \cot \varepsilon = k$$

$$- \frac{1}{2} \beta + \frac{\phi}{h} \cot (\phi - \varepsilon) = -k \tag{3.22}$$

Eliminating cot ε with the trigonometric formula for cot (ϕ−ε), we obtain

$$2 \phi \cot \phi = f(\phi)$$

$$f(\phi) = \frac{\beta^2 h^2/4 + \phi^2 - k^2 h^2}{kh} = \frac{\beta^2 h^2/4 + \phi^2}{kh} - kh \tag{3.23}$$

There is an infinite number of solutions ϕ_n (n = 1, 2, ...) of this transcendental equation. The smallest solution ϕ^2_{min} is always the most important one, for it generates the largest growth rate. We consider several limiting cases.

In the case of an almost sharp boundary layer kh → 0, but ßh finite, (3.23) becomes asymptotically.

$$\frac{1}{4} \beta^2 h^2 + \phi^2 \underset{kh \to 0}{\longrightarrow} 2\, kh \cdot \phi \cot \phi \tag{3.24}$$

$$\frac{1}{4} \beta^2 h^2 + \phi^2_{min} \approx 2\, kh \tag{3.25}$$

$$l_{min} \approx \frac{2\, kh}{\beta k^2 h^2} = \frac{1}{k} \frac{2}{\beta h} \approx \frac{1}{k} \frac{\rho_2 + \rho_1}{\rho_2 - \rho_1}$$

$$\sigma^2 \approx gk \frac{\rho_2 - \rho_1}{\rho_2 + \rho_1} \tag{3.26}$$

in accordance with (1.1).

For gradually decreasing kh a remarkable transition occurs. If

$$\frac{\beta^2 h^2}{4kh} - kh = 2 \quad \text{so that } f(\phi) = 2 + \frac{\phi^2}{kh} \tag{3.27}$$

or $$kh = kh_c = -1 + \sqrt{1 + \frac{1}{4} \beta^2 h^2} \approx \frac{1}{8} \beta^2 h^2 \lesssim \frac{1}{8} \tag{3.28}$$

it follows from (3.23) that $\phi^2_{min} = 0$ and hence also ε = 0. This means that if kh takes the critical value kh_c a solution of the form (3.19) cannot exist. There is, however, a suitable way for passing to the limits. Let

$$\frac{ß^2h^2}{4kh} - kh = 2 - \delta^2, \quad \delta \to 0 \tag{3.29}$$

so that kh is slightly larger than kh_c. Then

$$2\,(1 - \frac{1}{3}\,\phi^2_{min}) \approx 2\,\phi_{min} \cot \phi_{min} = 2 - \delta^2 + \frac{\phi^2_{min}}{kh}$$

$$\phi_{min} \approx \frac{1}{\sqrt{\frac{1}{kh} + \frac{2}{3}}}\,\delta \tag{3.30}$$

$$\phi_{min}\,\frac{1}{\varepsilon} \approx \phi_{min} \cot \varepsilon = -\,kh - \frac{1}{2}\,ßh$$

$$\varepsilon \approx -\,\frac{1}{kh + \frac{1}{2}\,ßh}\,\phi_{min} \tag{3.31}$$

$$\delta v_z \underset{kh \to kh_c}{\longrightarrow} \delta V\, e^{-1/2\; ßz} \sin\left[\phi_{min}\,\left(\frac{z}{h} + \frac{1}{kh + \frac{1}{2}\,ßh}\right)\right]$$

$$\delta v_z \underset{kh \to kh_c}{\longrightarrow} \delta V^{*}\, e^{-1/2\; ßz}\,\left(\frac{z}{h} + \frac{1}{kh + \frac{1}{2}\,ßh}\right) \tag{3.32}$$

If finally kh falls below kh_c we have $\phi^2_{min} < 0$ and hence $\phi_{min} = i\theta$, $\varepsilon = i\eta$. Consequently

$$\phi_{min} \cot \phi_{min} = \theta \cdot \mathrm{Cot}\,\theta, \; \phi_{min} \cot \varepsilon = \theta \cdot \mathrm{Cot}\,\eta \tag{3.33}$$

$$\delta v_z = \delta V\, e^{-1/2ßz} \sin i(\frac{\theta z}{h} - \eta) = \delta V^{*}\, e^{-1/2\; ßz}\, \mathrm{Sin}\,(\frac{\theta z}{h} - \eta) \tag{3.34}$$

We conclude therefore that the ordinary sine (3.19) is reduced for $kh = kh_c$ to a linear z-dependence (3.32) and for $kh<kh_c$ it is converted to the hyperbolic sine (3.34). $kh = kh_c$ may thus be regarded as defining the transition from the diffuse to the sharp boundary layer. In the limiting case of very large kh, equation (3.23) simplifies to $2\,\phi \cot \phi \approx -\,kh + \phi^2/kh$ with the solutions $\phi_n \approx n \cdot \pi$, the same as in the case of solid walls. We thus find that for short wave lengths it does not matter whether the boundary layer is confined by solid walls or by free surfaces.

A graphical solution of the transcendental equation (3.23) for ϕ is obtained by intersecting the different branches of the $2\,\phi\cot\phi$-curve with the parabola $f(\phi)$ (fig. 3). For $kh \gg kh_c$ the parabola starts far below and is very flat ($\phi_n \approx n\pi$), for $kh \searrow kh_c$ it is gradually displaced upwards and compressed, for $kh = kh_c$ the first intersecting point is reduced to $\phi_1 = 0$, until finally for $kh < kh_c$ it becomes imaginary, because then the parabola no longer intersects the first branch of $2\,\phi\cot\phi$ in the real plane.

This completes the treatment of the problem of hydrodynamic stability of a diffuse boundary layer in the absence of dynamic stabilization. We have derived the growth rates and eigenfunctions by modifying and extending the original considerations of Lord Rayleigh.

3.2 Dynamic Stabilization

3.2.1 Reduction to Mathieu's Equation

We next turn to a system subject to forced oscillations parallel to the direction of the gravity with acceleration $\vec{g}$. The stability of this dynamical system has been theoretically investigated by Wesson /4/. In the following, we reconsider and carry on his essential ideas and procedures. Let

$$\gamma(t) = g + b(t) = g + b_0 \cos \omega t \tag{3.35}$$

be the acceleration in the frame of reference moving with the fluid. Then in the equation of motion g must be replaced by $\gamma(t)$, and a Fourier decomposition $e^{i\Omega t}$ is no longer possible. We must retain the derivative $\partial/\partial t$ when eliminating the perturbed quantities from (3.1) to (3.3), and obtain the following equations for $\delta\rho/\rho$ and δv_z:

$$k^2\gamma(t)\,\frac{\delta\rho}{\rho} - \left[\frac{1}{\rho}\frac{\partial}{\partial z}\left(\rho\,\frac{\partial}{\partial z}\right) - k^2\right]\frac{\partial}{\partial t}\,\delta v_z = 0 \tag{3.36}$$

$$\frac{\partial}{\partial t}\frac{\delta\rho}{\rho} + \frac{\rho'}{\rho}\,\delta v_z = 0 \tag{3.37}$$

Defining $\rho'/\rho = \beta$, we can eliminate δv_z:

$$ßk^2 \ \gamma(t) \ \frac{\delta\rho}{\rho} + \left[\frac{1}{\rho}\frac{\partial}{\partial z}(\rho\frac{\partial}{\partial z}) - k^2\right] \frac{\partial^2}{\partial t^2}\frac{\delta\rho}{\rho} = 0 \tag{3.38}$$

The separation of variables by

$$\frac{\delta\rho}{\rho}(z,t) = \frac{\delta\rho}{\rho}(z) \cdot X(t), \ \delta v_z(z,t) = \delta v_z(z)\cdot\Phi(t) \tag{3.39}$$

leads to

$$\frac{\left[\frac{1}{\rho}\frac{d}{dz}(\rho\frac{d}{dz}) - k^2\right]\frac{\delta\rho}{\rho}(z)}{ß\frac{\delta\rho}{\rho}(z)} = -k^2\gamma(t)\frac{X(t)}{\frac{d^2}{dt^2}X(t)} \tag{3.40}$$

The left hand side depends only on z , the right one only on t, so both are equal to the same separation constant. We call it k^2g/Ω^2 and obtain

$$\left[\frac{1}{\rho}\frac{d}{dz}(\rho\frac{d}{dz}) - k^2\right]\frac{\delta\rho}{\rho}(z) = \frac{k^2gß}{\Omega^2}\frac{\delta\rho}{\rho}(z) \tag{3.41}$$

$$-\gamma(t) \ X(t) = \frac{g}{\Omega^2}\frac{d^2}{dt^2}X(t) \tag{3.42}$$

Equation (3.41) has the same form as (3.4) and leads to a boundary value problem in z, (3.42) to an initial value problem in t. Because of

$$\frac{\partial}{\partial t}\frac{\delta\rho}{\rho}(z,t) + ß\delta v_z(z,t) = \frac{\delta\rho}{\rho}(z)\frac{d}{dt}X(t) + ß\delta v_z(z) \ \Phi(t) = 0$$

or

$$\frac{\frac{\delta\rho}{\rho}(z)}{\delta v_z(z)} = -ß\frac{\Phi(t)}{\frac{d}{dt}X(t)} = \text{const} \tag{3.43}$$

the relative perturbed density $\delta\rho/\rho$ (z) is proportional to the pèrturbed velocity $\delta v_z(z)$. By normalizing the proportionality constant to unity, the boundary conditions (3.18) for δv_z are transferred to $\delta\rho/\rho$. This boundary value problem has already been solved in chapter 3.1.2. The separation constant is the eigenvalue parameter and takes the form

$$\frac{g}{\Omega^2} = -1 = -1_{mn} = -\frac{ß^2h^2/4 + \phi^2_{mn} + k^2_m h^2}{ßk^2_m h^2} \tag{3.44}$$

$$m,n = 1, 2, 3, \ldots$$

and the differential equation for X(t) becomes

$$\frac{d^2}{dt^2} X(t) = \frac{\gamma(t)}{l} X(t) = \frac{g+b_o \cos \omega t}{l} X(t) \tag{3.45}$$

Let $\tau = \frac{\omega t}{2}$, $\chi(\tau) = X(t)$. Then

$$\frac{d^2}{d\tau^2} \chi(\tau) - \frac{4}{\omega^2} \frac{g+b_o \cos 2\tau}{l} \chi(\tau) = 0 \tag{3.46}$$

or with

$$\boxed{\begin{aligned} &\ddot{\chi}(\tau) + (a - 2 q \cos 2 \tau) \chi(\tau) = 0 \\ &a = -\frac{4 g}{\omega^2 l} = \frac{4 \Omega^2}{\omega^2} = -\frac{4 \sigma^2}{\omega^2} \\ &q = \frac{2 b_o}{\omega^2 l} = \frac{b_o}{2g} \frac{4 g}{\omega^2 l} = -\frac{b_o}{2g} a \end{aligned}} \tag{3.47}$$

The equation 3.47 for $\chi(\tau)$ is Mathieu's differential equation. We need solutions of this equation in the fourth quadrant of the (q,a)-plane, along the straight lines

$$a = - cq = -\frac{2g}{b_o} q, \qquad q > 0 \tag{3.48}$$

$\sqrt{-a}$ is the growth rate in the static system ($b_o = 0 = q$), measured in units of the forced oscillation frequency in the dynamic system. The slope c of the straight line is given by the ratio of the gravity acceleration to the amplitude of the acceleration of the forced oscillation. The present problem is mathematically identical with the problem of dynamic stabilization of an inverted pendulum of length l by shaking vertically the point of support. The only but crucial difference consists in the fact that in a liquid the length l of the pendulum is replaced by an infinite matrix of values l_{mn} corresponding to the mode number combinations m, n.

3.2.2 Stability Condition and Growth Rates

A complete stabilization would be achieved only if all admissible values of l could be stabilized simultaneously. However, this is principally impossible as is shown clearly by Mathieu's stability diagram (fig. 4).

Stability exists only for parameter sets (q, a) within the hatched region between the curve $a_o(q)$, parabolic near the origin, and the curve $b_1(q)$, intersecting the q-axis at q_s. The proper parameter of the straight line a = - cq is the reciprocal pendulum length l, and the final point is characterized by the minimum possible length l_{min}. According to (3.44) it is

$$l_{min} = \lim_{k_m \to \infty} l = \frac{1}{ß} \tag{3.49}$$

By choosing a sufficiently high shake frequency ω one can always move the end point of the straight line into the stability region and thus avoid the region of parametric instabilities above $b_1(q)$, but the instability region below $a_o(q)$ must always be crossed by the straight a = -cq, even for arbitrarily small c. Consequently large vertical mode numbers n, corresponding to short vertical wave lengths $\lambda_\perp$, cannot be completely dynamically stabilized. The unstable solutions of the Mathieu equation have the form $e^{\mu\tau} f(\tau)$, where $f(\tau)$ may be represented by a series expansion in sine- and cosine-functions of different periodicity. The theory of Mathieu functions has been developped in the text books of Meixner-Schäfke /5/ and McLachlan /6/. Some approximate formulae for the pertinent stability boundaries and growth rates of the Mathieu chart, taken from the text books, have been collected and reformulated for our purposes in /7/. They provide analytic expressions for the calculation of the growth rate $\mu(q,a)>0$ in the two relevant instability regions. The functions $\mu(q, -cq)$ have been calculated for c = 0.1, 0.2, ..., 0.5, and the results are plotted in fig. 5. The instability region at small q, as well as the maximum growth rate in this region, both shrink proportional to decreasing c. However, when entering the region of parametric instabilities, it is sufficient to exceed the stability limit $b_1(q)$ by a small amount in q in order to generate very large growth rates μ. We shall need only the small growth rates in the first instability region and take from /7/ the following approximate formulae for small q and small c:

$$a_o(q) = -\frac{1}{2} q^2 \;, \quad \mu^2(q,a) = - a - \frac{1}{2} q^2 \tag{3.50}$$

Using (3.47) μ^2 may also be written as

$$\mu^2 = - a - \frac{1}{2} \frac{b_o^2}{4 g^2} a^2 = - a \left(1 + \frac{b_o^2}{8g^2} a\right) \tag{3.50}$$

$$\mu^2 = \frac{4 \sigma^2}{\omega^2} \left(1 - \frac{b_o^2}{g^2} \frac{\sigma^2}{2 \omega^2}\right) \tag{3.51}$$

For the intersection point q_o of $a = -cq$ with $a = a_o(q)$ it follows

$$- cq_o = - \frac{1}{2} q_o^2 , \quad q_o = 2 c \tag{3.52}$$

and for the maximum growth rate μ_{max} and the associate q_{max} it results

$$\mu^2 (q, -cq) = cq - \frac{1}{2} q^2, \frac{d}{dq} \mu^2 = c-q$$

$$q_{max} = c \quad , \quad \mu^2_{max} = \frac{1}{2} c^2 \tag{3.53}$$

In the neighbourhood of the zero q_s the curve $b_1(q)$ may be approximated by its tangent

$$b_1(q) = \left.\frac{db_1}{dq}\right|_{q_s} \cdot (q-q_s) = - 1.191 \ (q-0.908) \tag{3.54}$$

Hence it follows for the intersection point q_{par} of $a = -cq$ with $a = b_1(q)$

$$cq_{par} = 1.191 \ (q_{par} - 0.908) , \quad q_{par} = \frac{0.908}{1 - \frac{c}{1.191}} \tag{3.55}$$

The stability condition may now briefly be written as

$$q_o < q < q_{par} \tag{3.56}$$

By inspection of (3.51) the relation $q_o < q$ can be brought into the form presented by Wolf /2/:

$$\frac{b_o^2}{g^2} > \frac{2 \omega^2}{\sigma^2} \tag{3.57}$$

The above derived formulae constitute a simple stability theory for the analysis of the behaviour of a dynamically stabilized diffuse boundary layer. For the case of a moderate density step the assumed exponentially increasing density profile can be approximated by a linear density distribution with sufficient accuracy.

4. Comparison of Theory and Experiment

We start from the following experimental parameters /2/:

Density of light fluid	$\rho_1 = 1.0\ g/cm^2$
Density of heavy fluid	$\rho_2 = 1.8\ g/cm^3$
Diameter of cylindrical vessel	$D = 0.78$ cm
Length of cylindrical vessel	$\Lambda = 6.0$ cm
Oscillation frequency	$\omega = 2\pi \cdot 10^2/sec$
Amplitude of oscillator acceleration	$b_o = 60$ g

From the oscillator acceleration we find immediately the slope of the straight line $a = -cq$ in the Mathieu chart. We have

$$c = \frac{2g}{b_o} = \frac{1}{30} \tag{4.1}$$

Hence the different q-values that characterize the stability behaviour are

$$q_{max} = c = \frac{1}{30}\ ,\ q_o = 2c = \frac{1}{15}\ , \quad q_{par} = \frac{0.908}{1 - \frac{c}{1.191}} = 0.934 \tag{4.2}$$

and the maximum growth rate in the first instability region is

$$\mu_{max} = \frac{1}{2}\sqrt{2}\ c = 0.02357 \tag{4.3}$$

Defining T by $e^{\mu\tau} = e^{\mu\omega t/2} = e^{t/T}$ the minimum e-folding time T_{min} of a perturbation turns out to be

$$T_{min} = \frac{2}{\mu_{max}\omega} = 0.135\ \text{sec} \tag{4.4}$$

If the boundary layer is initially quite sharp, short wave length modes with large k can grow nearly arbitrarily fast according to (1.1). As a consequence the adjacent fluid layers of different density get mixed, and the density step is transformed into a steady density profile, at first still with a very steep local density increase. The relative density gradient $\beta = \rho'/\rho$ determines the end point of the straight line $a = -cq$ in fig. 4. As long as this end point remains in the region of parametric instabilities, perturbations with sufficiently large k values will continue to grow. Although their growth will no longer be arbitrarily fast, their growth rates μ, as shown in fig. 5, are still about 10 to 20 times larger than μ_{max} as calculated from equ. (4.3). The associate growth times T are of the order of 10 msec, so that the density gradient must be flattened almost instantaneously until the endpoint of $a = -cq$ arrives at the stability boundary $b_1(q)$, and q_{end} no longer exceeds q_{par}. We conclude that the parametric instabilities manifest themselves by fixing an upper bound β_{par} for the admissible density gradient, but in general they cannot occur visibly in the experiment. Inserting numbers we find

$$q_{end} = \frac{2}{\omega^2}\,\frac{b_o}{l_{min}} = \frac{2}{\omega^2}\,b_o\beta \rightarrow q_{par}$$

$$\beta_{par} = \frac{\omega^2\,q_{par}}{2\,b_o} = \frac{4\pi^2\cdot 10^4\cdot 0.934}{2.60\cdot 981\cdot \mathrm{cm}} = \frac{3.13}{\mathrm{cm}} \qquad (4.5)$$

In the following density profiles with $\beta \leq \beta_{par}$ are examined in detail.

4.1 Phase I: Formation of Stairs

From β_{par} follows a minimum boundary layer thickness h_{par}. It is

$$\frac{\rho_2}{\rho_1} = e^{\beta h}\ , \quad h_{par} = \frac{1}{\beta_{par}}\ln\frac{\rho_2}{\rho_1} = \frac{\ln 1.8}{3.13} = 0.188\ \mathrm{cm} \qquad (4.6)$$

When treating Rayleigh-Taylor instabilities the quantity kh is most important. In the experiment kh cannot become smaller than $k_{min}\,h_{par}$ with

$$k_{min} = \frac{2\pi}{\lambda_{max}} = \frac{3.68}{D} = \frac{3.68}{0.78} = \frac{4.72}{\mathrm{cm}} \qquad (4.7)$$

hence $k_{min}\,h_{par} = 0.887$ (4.8)

On the other hand the critical kh_c defined by (3.28) is

$$kh_c \approx \frac{1}{8}\,\beta^2 h^2 = \frac{1}{8}\left(\ln\frac{\rho_2}{\rho_1}\right)^2 = 0.043 \qquad (4.9)$$

We are therefore always in the limiting case $kh \gg kh_c$ and calculate the ϕ_n from the equation

$$2\ \phi\ \cot\ \phi\ =\ f(\phi)\ =\ -\ kh\ +\ \frac{\phi^2}{kh} \tag{4.10}$$

For $kh = k_{min} h_{par} \approx 1$ one could plot a corresponding $f(\phi)$-curve in fig. 3 and find that $\phi_1 < \pi/2$ and

$$\phi_n \approx (n-1)\ \pi \quad \text{for} \quad n = 2,\ 3,\ \ldots \tag{4.11}$$

Iteration yields the first solution of the transcendental equation with the result

$$\phi_1 \approx 1.241 \tag{4.12}$$

We now consider the equivalent pendulum length

$$l_n \approx \frac{1}{\beta_{par}} \frac{\phi_n^2 + k_{min}^2 h_{par}^2}{k_{min}^2 h_{par}^2} \tag{4.13}$$

and calculate q_n- and μ_n-values for the different vertical mode numbers n.

$$q_n = \frac{2b_o}{\omega^2 l_n} = q_{par} \frac{k_{min}^2 h_{par}^2}{\phi_n^2 + k_{min}^2 h_{par}^2} = \frac{0.735}{\phi_n^2 + 0.787} \tag{4.14}$$

$$\mu_n = \sqrt{c\ q_n - \frac{1}{2} q_n^2} = \sqrt{\frac{1}{30} q_n - \frac{1}{2} q_n^2} \tag{4.15}$$

The results are collected in

Table 1

n	ϕ_n	q_n	μ_n
1	1.241	0.3158	0
2	π	0.0690	0
0	-	$0.0667 = \frac{1}{15}$	0
max	-	$0.0333 = \frac{1}{30}$	0.0236
3	2π	0.0183	0.0210
4	3π	0.0082	0.0155

Here we have included the indices n = 0 (stability boundary) and n = max (maximum growth rate). Clearly the modes n = 1 and n = 2 are dynamically stabilized, but all higher modes are not. The mode n = 3 has the largest growth rate. When its amplitude has grown to a certain amount, its velocity field changes the density profile. This violates the conditions for a further growth, and finally the mode must decay and disappear by nonlinear effects. We can extrapolate from the linear velocity field to the nonlinear final state. According to (3.19) we have

$$\delta v_z = \delta V \; e^{-1/2\, \beta_{par} z} \sin \left(\frac{\phi_3 z}{h_{par}} - \varepsilon_3\right) \tag{4.16}$$

with $\phi_3 \approx 2\pi$, and where ε_3 from (3.22) is the solution of the equation

$$\phi_3 \cot \varepsilon_3 = -k_{min} h_{par} - \frac{1}{2} \beta_{par} h_{par} \tag{4.17}$$

Using (4.6) and (4.8) we obtain $\varepsilon_3 = -1.385 \approx -\pi/2$, so that (4.16) takes approximately the form

$$\begin{aligned} \delta v_z &= \delta V \; e^{-1/2\, \beta_{par} z} \sin \left(\frac{2\pi z}{h_{par}} + \frac{\pi}{2}\right) \\ &= \delta V \; e^{-1/2\, \beta_{par} z} \cos \frac{2\pi z}{h_{par}} \end{aligned} \tag{4.18}$$

The cosine dependence follows from the fact that the two limiting surfaces of the boundary layer can oscillate freely because of the absence of solid walls. The factor $e^{-1/2\, \beta_{par} z}$ is approximately equal to 1. For $z > h_{par}$ the amplitude decays according to (3.17) and (4.8) as $e^{-k_{min} z} = e^{-0.877\, z/h_{par}}$, and the equivalent holds for $z<0$. Thus above and below the boundary layer, adjacent liquid layers of about the thickness h_{par} of the boundary layer itself are affected by the motion. Schematically these results are illustrated in fig. 6a. It should be noted that the z-direction has been expanded by a factor ≈2 relative to the x-direction, $h_{par} \approx 2$ mm compared with D ≈ 8 mm. The velocity field shows three linked eddies, each one with the tendency to flatten the density profile within its region of influence. Hence three intermediate plateaus will be created, and the nonlinear final state of the density profile exhibits a sequence of stairs with four steps as shown in fig. 6b, the steepness of each step being limited to β_{par} because of the activity of the parametric instabilities. Obviously the two outer steps are more liable to breakdown and will get smoothed out earlier than the two inner steps. The time $t_2 - t_1$ needed for the formation of the stairs structure will exceed the growth time T_{min} (4.4) by an order of magnitude. All these results are in good agreement with the experimental observations.

4.2 Phase II: Periodical Sheet Detachment

The four stair steps, after their formation, will exist independently, and we now consider the time development of each single step.
Let

$$\tilde{\rho}_1 = 1.4 \text{ g cm}^{-3}, \quad \tilde{\rho}_2 = 1.6 \text{ g cm}^{-3}, \tag{4.19}$$

the tilde referring to quantities characterizing the diffusion process at the chosen single step. The minimum boundary layer thickness is now given by

$$\tilde{h}_{par} = \frac{1}{\beta_{par}} \ln \frac{\tilde{\rho}_2}{\tilde{\rho}_1} = \frac{1}{3.13} \ln \frac{1.6}{1.4} = 0.0427 \text{ cm} \approx \frac{1}{2} \text{ mm} \tag{4.20}$$

and further

$$k_{min} \tilde{h}_{par} = 4.72 \times 0.0427 = 0.202 \tag{4.21}$$

$$k\tilde{h}_c \approx \frac{1}{8} \tilde{\beta}^2 \tilde{h}^2 = \frac{1}{8} (\ln \frac{\tilde{\rho}_2}{\tilde{\rho}_1})^2 = 0.00223 << k_{min} \tilde{h}_{par} \tag{4.22}$$

For $kh = k_{min} \tilde{h}_{par}$ the equation (4.10) has the solutions

$$\phi_1 \approx 0.625, \quad \phi_n \approx (n-1)\, \pi \text{ for } n \geq 2 \tag{4.23}$$

We now consider in addition to the vertical mode numbers n also the horizontal mode numbers m, and for sake of simplicity we put $k_m = m \cdot k_{min}$ as in the case of rectangular vessel cross section. For our purposes the error for m>1 does not matter. We then have

$$q_{mn} = q_{par} \frac{m^2 k_{min}^2 \tilde{h}_{par}^2}{\phi_{mn}^2 + m^2 k_{min}^2 \tilde{h}_{par}^2}$$

$$q_{mn} = \frac{0.0381 \, m^2}{\phi_{mn}^2 + 0.0408 \, m^2}, \quad \mu_{mn} = \sqrt{\frac{1}{30} q_{mn} - \frac{1}{2} q_{mn}^2} \tag{4.24}$$

and the following approximate numbers

$$\phi_{11} = 0.63,\ \phi_{21} = 0.87,\ \phi_{31} = 1.05,\ \phi_{41} = 1.19$$

$$\phi_{mn} = (n-1)\ \pi \text{ for } n \geq 2,\ m = 1,2,3,4 \tag{4.25}$$

From (4.24) and (4.25) there results for the number pairs q_{mn}/μ_{mn} the

Table 2

m →	1		2		3		4	
n ↓	q	μ	q	μ	q	μ	q	μ
1	0.087	0.0	0.166	0.0	0.233	0.0	0.295	0.0
2	0.0038	0.0110	0.0152	0.0198	0.0335	0.0236	0.0579	0.0159
3	0.0010	0.0056	0.0038	0.0110	0.0086	0.0158	0.0152	0.0198
4	0.0004	0.0038	0.0017	0.0075	0.0038	0.0110	0.0068	0.0143

Evidently modes with n = 1 are always dynamically stabilized. Thus the ground mode is the mode m = 1, n = 2. Since its growth rate is small compared with the growth rates of numerous higher modes, it cannot be observed from the beginning. However, the competing higher modes destroy each other, cause some turbulent diffusion, and hence lead to a gradual increase of the boundary layer thickness $\tilde{h}$ as well as a decrease of the relative density gradient $\tilde{\beta}$, the product $\tilde{\beta}(t)\ \tilde{h}(t) = \beta_{par}\ \tilde{h}_{par}$ remaining constant. But for small m and small $n \geq 2$ it is

$$q_{mn} \approx q_{par} \frac{m^2 k^2_{min}\ \tilde{h}^2_{par}}{(n-1)^2 \pi^2} = \frac{2b_o}{\omega^2} \frac{\beta_{par}\ \tilde{h}^2_{par}\ m^2\ k^2_{min}}{(n-1)^2 \pi^2}$$

so that

$$q_{mn}(t) \approx \frac{2b_o}{\omega^2} \frac{\beta_{par}\ \tilde{h}_{par}\ m^2\ k^2_{min}}{(n-1)^2 \pi^2}\ \tilde{h}(t) \tag{4.26}$$

In the same measure as $\tilde{h}$ is increased, the q_{mn} are shifted and hence the associate μ_{mn} as well. Whereas in Table 2, at a time $t = t_o$, the mode m = 3, n = 2 has the highest growth rate, with increasing $\tilde{h}$ this mode must be superseded at first by the mode m = 2, n = 2, until finally the ground mode m = 1, n = 2 wins through. For this it is not necessary that q_{12} be equal to q_{max}, because the $\mu(q)$-curve is so flat near its maximum that already q_{12}-values are sufficient which correspond to an increase of the sheet thickness from $\tilde{h}_{par}$ to about h_{par}, i.e. from about 1/2 mm to the initial 2 mm.

We call this time $t = t_1$ and have

$$q_{12}(t_1) = q_{12}(t_o) \frac{h_{par}}{\tilde{h}_{par}} = 0.00384 \frac{0.188}{0.0427} = 0.0169$$

$$\mu_{12}(t_1) = 0.0205 \tag{4.27}$$

It is to be noted that $q_{m2}(t_1) > q_o$ for $m \geq 2$, i.e. these modes are then dynamically stabilized. Moreover

$$\delta v_z(z,t_1) = \delta V e^{-1/2 \tilde{\beta}(t_1)z} \sin \left(\frac{\phi_{12} z}{h_{par}} - \varepsilon_{12}\right) \tag{4.28}$$

where $\phi_{12} \approx \pi$ and ε_{12} is solution of

$$\phi_{12} \cot \varepsilon_{12} = -k_{min} h_{par} - \frac{1}{2} \ln \frac{1.6}{1.4} = -0.954$$

$$\varepsilon_{12} = -1.276 \approx -\pi/2 \tag{4.29}$$

Thus with sufficient accuracy the volocity is similar to eq. (4.18)

$$\delta v_z \approx \delta V e^{-1/2 \tilde{\beta} z} \cos \frac{\pi z}{h_{par}} \tag{4.30}$$

Schematically the situation is illustrated by fig. 7a, showing a velocity field with two linked eddies. The lower one transports lighter fluid into the boundary layer, the upper one heavier fluid. Thus the density step is steepened again, the slope remaining bounded by β_{par}. At the same time the lighter fluid, that has been transported upwards by the upper eddy, loses contact with the boundary layer, and the same happens to the heavier fluid, that has been transported downwards by the lower eddy. Mind that this time the step gradient is much flatter, at $t = t_1$ it is $\tilde{\beta} \approx \frac{1}{4} \beta_{par}$ (fig. 7b). Hence the eddies produce not only a density equalization but even a local reversal in gradient. At time $t = t_2$ a sheet of relatively high density is peeled off downwards and a sheet of relatively low density upwards. Both are free to move independently, the compression sheet following the gravity and the rarefaction sheet following the buoyancy. At time $t = t_3$ the slow flattening of the density profile starts again, according to the turbulent diffusion caused by the higher modes. The interval $t_3 - t_o$ ($\gg t_3 - t_1$) defines the period length. The macroscopically visible effect of detachment of thin sheets is periodically repeated by the intermittent appearance of a far-reaching convection of the ground mode. When arriving at neighbouring steps, the density and rarefaction sheets produce there a steepening of the density profiles. Also the distance of the steps from each other is enlarged. If on the other hand a compression sheet and a rarefaction sheet encounter each other they will be annihilated. In this case the distance of neighbouring steps remains unchanged. In summary, we may state that all the experimentally observed phenomena of anomalous diffusion have a clear theoretical interpretation.

5 Nonlinear Theory for the Maximum Convective Transport by Quasistationary Vortex Flow

We have seen that a dynamically stabilized diffuse boundary layer decays into a sequence of stairs, with up to four steps in the case of Wolf's /2/ experiment. This stairs formation is a transient process and shall not be investigated further in the following. Each single step displays a periodical sheet detachment produced by two linked fluid vortices or convective cells. These eddies can be formed only if the density gradient in the boundary layer is such that the ground mode grows faster than the competing modes. In general this most favourable gradient for the ground mode is smaller than the maximum gradient prescribed by the parametric instabilities. So it takes some time until by ordinary diffusion and by higher mode induced microturbulence the density profile is sufficiently flattened for allowing the ground mode to dominate. Hence the convection is not continuous but intermittent. A theoretical description would be difficult, because the transport depends mainly on the long quiescent phases between successive sheet detachments, where the effective diffusion coefficient is unknown. If, however, the experimental conditions are chosen in such a way that the parametrically determined density gradient is optimal for the excitation of the ground mode, then a stationary vortex flow is maintained and the convection cells persist for a long time. The amplitude of the vorticity is finally limited by nonlinear effects, and the saturation amplitude determines the maximum possible convective transport. In the following we treat this quasistationary limiting case and extend the analysis of the linear modes into the nonlinear regime. It will turn out that the stationary motion is superposed by periodic oscillations with the shake frequency, so that the term quasistationary is more appropriate.

For a quantitative formulation of the basic assumptions, we remember that the linear modes are represented by points in the Mathieu chart (fig. 4) situated along the straight line $a = -2g/b_o\, q$, that terminates at $q = q_{end}$. For $q = q_{max} = q_o/2$ the growth rate is maximal, and for $q \leq q_{par}$ the parametric instabilities are suppressed. The expressions are

$$q_{end} = \frac{2\, b_o \beta}{\omega^2}\ , \quad q_{max} = \frac{2g}{b_o}\ , \quad q_{par} = \frac{0.908}{1 - \frac{2\, g}{1.191\, b_o}} \qquad (5.1)$$

We suppose $2g/b_o << 1$, then q_{par} is almost constant. The (m,n)-mode is characterized up to very small corrections by

$$q_{mn} = \frac{2\ b_o \beta}{\omega^2} \frac{m^2 k^2_{min} h^2}{(n-1)^2 \pi^2 + m^2 k^2_{min} h^2} = \frac{2\ b_o \beta}{\omega^2} \frac{m^2 h^2}{(n-1)^2\ D^2 + m^2 h^2} \tag{5.2}$$

where D denotes the longer side of a rectangular vessel cross section. We don't care here for the modifications in the cylindrical case. The ground mode m = 1, n = 2 dominates if q_{12} tends to q_{max}, hence our first requirement is

$$\frac{2\ b_o \beta}{\omega^2} \frac{h^2}{D^2+h^2} = \frac{2g}{b_o} \tag{5.3}$$

In addition we require that the relative density gradient $\beta = \rho'/\rho \approx \Delta\rho/h\rho$ has its maximum value determined by the parametric resonances, so that q_{end} coincides with q_{par}:

$$\frac{2\ b_o \beta}{\omega^2} = \frac{0.908}{1 - \frac{2\ g}{1.191\ b_o}} \tag{5.4}$$

If the conditions (5.3) and (5.4) are simultaneously fulfilled, the periodically intermittent sheet detachment becomes quasicontinuous, thus increasing considerably the convective mass throughput. For given ß, h, D the shake parameters ω and b_o may always be chosen properly. Indeed such conditions have been realized in experiments by Hopmann et al. /3/, which showed very impressively the formation of stationary (duration ∿1 min) vortex motion with two linked convective cells. Our nonlinear theory is intended to yield the mean convective mass current density in the quasistationary limiting case as an upper bound for the possible mass transport.

5.1 Reduction of the System of Basic Equations

To find the relevant nonlinear terms we must go back to the original system of hydrodynamic equations:

$$\rho \frac{d\vec{v}}{dt} = \rho(\frac{\partial}{\partial t} + \vec{v}\cdot\nabla)\ \vec{v} = -\nabla p + \rho\vec{g} \tag{5.5}$$

$$\frac{d\rho}{dt} = (\frac{\partial}{\partial t} + \vec{v}\cdot\nabla)\ \rho = \frac{\partial\rho}{\partial t} + \nabla\cdot(\rho\vec{v}) = 0 \tag{5.6}$$

$$\nabla\cdot\vec{v} = 0 \tag{5.7}$$

with $\vec{g} = -\gamma(t)\ \vec{e}_z = -(g + b_o \cos \omega t)\ \vec{e}_z$ (5.8)

We consider only cases in which the amplitude b_o of the enforced harmonic acceleration is much larger than the gravity acceleration g. If the boundary layer is initially at rest, we may introduce perturbed quantities by

$$\vec{v} \to \delta\vec{v}, \qquad \rho \to \rho + \delta\rho, \qquad p \to p + \delta p$$

with $\rho = \rho(z) = \rho_o\ e^{\beta z}$, $0 \leq z \leq h$ (5.9)

and $\quad -\nabla p + \rho\vec{g} = 0$

Using the relative density perturbation $\delta\rho/\rho$ instead of $\delta\rho$ we get the following perturbed equations:

$$(1 + \frac{\delta\rho}{\rho})\ (\frac{\partial}{\partial t} + \delta\vec{v}\cdot\nabla)\ \delta\vec{v} = -\frac{1}{\rho}\nabla\delta p + \frac{\delta\rho}{\rho}\vec{g} \tag{5.10}$$

$$(\frac{\partial}{\partial t} + \delta\vec{v}\cdot\nabla)\ \frac{\delta\rho}{\rho} = -\ \beta\ (1 + \frac{\delta\rho}{\rho})\ \delta v_z \tag{5.11}$$

$$\nabla\cdot\delta\vec{v} = 0 \tag{5.12}$$

In either eddy the density variation $\delta\rho$ must be less than half the density step $\Delta\rho$ at the boundary layer:

$$\frac{\delta\rho}{\rho} < \frac{1}{2}\frac{\Delta\rho}{\rho} \approx \frac{1}{2}\beta h << 1 \tag{5.13}$$

We restrict our analysis to relative density variations which are small compared with unity. Furthermore we consider only vessels with rectangular cross section and with one side being much longer than the other. If then the longer side of the rectangle denotes the x-direction and the shorter one the y-direction, the modes in the y-direction have a much shorter wavelength and need not be taken into account for macroscopic motions. This makes the problem purely twodimensional, and reduces the velocity to

$$\delta\vec{v} = \delta v_x \vec{e}_x + \delta v_z \vec{e}_z \tag{5.14}$$

With these simplifications (5.10) becomes

$$\left(\frac{\partial}{\partial t} + \delta\vec{v}\cdot\nabla\right)\begin{pmatrix}\delta v_x \\ \delta v_z\end{pmatrix} = -\frac{1}{\rho}\begin{pmatrix}\frac{\partial}{\partial x}\,\delta p \\ \frac{\partial}{\partial z}\,\delta p\end{pmatrix} + \frac{\delta\rho}{\rho}\begin{pmatrix}0 \\ -\gamma\end{pmatrix} \tag{5.15}$$

From (5.12) and (5.14) we derive the relations

$$\frac{\partial}{\partial z}\,(\delta\vec{v}\cdot\nabla)\,\delta v_x = (\delta\vec{v}\cdot\nabla)\,\frac{\partial}{\partial z}\,\delta v_x \tag{5.16}$$

$$\frac{\partial}{\partial x}\,(\delta\vec{v}\cdot\nabla)\,\delta v_z = (\delta\vec{v}\cdot\nabla)\,\frac{\partial}{\partial x}\,\delta v_z$$

Eliminating δp and applying (5.16) the equations (5.15) and (5.11) are reduced to

$$\left(\frac{\partial}{\partial t} + \delta\vec{v}\cdot\nabla\right)\left(\beta\delta v_x + \frac{\partial}{\partial z}\,\delta v_x - \frac{\partial}{\partial x}\,\delta v_z\right) = \gamma(t)\,\frac{\partial}{\partial x}\,\frac{\delta\rho}{\rho} \tag{5.17}$$

$$\left(\frac{\partial}{\partial t} + \delta\vec{v}\cdot\nabla\right)\frac{\delta\rho}{\rho} = -\beta\delta v_z \tag{5.18}$$

Obviously the only difference to the linear theory is the occurrence of the additional convective term $\delta\vec{v}\cdot\nabla$. This term causes the nonlinear saturation. For sufficiently large $\delta\vec{v}$ the exponential growth of modes is impeded, and a stationary flow is formed. For solving the system (5.17) and (5.18) of coupled nonlinear equations, we write the perturbed quantities as series expansions in the well-known linear modes:

$$\left.\begin{matrix}\delta v_z \\ \\ \delta\rho/\rho\end{matrix}\right\} = e^{-1/2\,\beta z}\sum_{m=1}^{\infty}\sum_{n=2}^{\infty}\left\{\begin{matrix}\delta V_{m,n-1}(t) \\ \\ \delta S_{m,n-1}(t)\end{matrix}\right\}\cos\frac{m\pi x}{D}\,\cos\frac{(n-1)\pi z}{h} \tag{5.19}$$

The summation excludes modes with $n=1$ because the linear theory showed that these modes have vanishing growth rates. The expansion (5.19) can be used within the boundary layer $0 \leq z \leq h$. The $\cos\frac{(n-1)\pi z}{h}$ -dependence describes standing waves with maxima at both free edges. We ignore the slight phase shifts that ensure steady transition to exponential decay beyond the upper and lower limiting surfaces. From δv_z we calculate

$$\delta v_x = \int dx \frac{\partial}{\partial x} \delta v_x = \int dx \left(- \frac{\partial}{\partial z} \delta v_z\right) \text{ as well as}$$

$\frac{\partial}{\partial z} \delta v_x$ and $\frac{\partial}{\partial x} \delta v_z$, and find

$$ß\delta v_x + \frac{\partial}{\partial z} \delta v_x - \frac{\partial}{\partial x} \delta v_z = - \frac{\partial}{\partial x} e^{-1/2\, ßz} \sum_{m=1}^{\infty} \sum_{n=2}^{\infty} \delta V_{m,n-1}(t)\; ß1_{mn} \cdot$$

$$\cdot \cos \frac{m\pi x}{D} \cdot \cos \frac{(n-1)\pi z}{h} \tag{5.20}$$

$$\text{with} \quad ß1_{mn} = \frac{\frac{ß^2}{4} + \frac{(n-1)^2\pi^2}{h^2} + \frac{m^2\pi^2}{D^2}}{\frac{m^2\pi^2}{D^2}} = \frac{2\, b_o ß}{\omega^2} \frac{1}{q_{mn}} \tag{5.21}$$

Considering only those linear modes, which are able to compete with the ground mode, we have to take into account q_{mn}-values near q_{12}:

$$q_{mn} \approx \frac{2\, b_o ß}{\omega^2} \frac{m^2 h^2}{(n-1)^2 D^2 + m^2 h^2} \approx \frac{2\, b_o ß}{\omega^2} \frac{h^2}{D^2+h^2} \approx q_{12} = q_{max} = \frac{q_o}{2} \tag{5.22}$$

Obviously $q_{mn} = q_{12}$ for $n-1 = m$. For simplicity we call these modes "pure", and modes with $n-1 \neq m$ "mixed". For low mode numbers $m, n \lesssim 4$, the q_{mn} of the mixed modes are very different from q_{12}. Hence the corresponding growth rates are noticeably smaller than the growth rate of the ground mode, or they even vanish completely. Therefore the lower mixed modes can be neglected. Modes with high mode numbers, on the other hand, whether they are pure or mixed, cannot be seen in the macroscopic convection, they only produce a slow diffusion by small-scale turbulence just as in the quiescent phases of the periodic sheet detachment. In addition, the higher modes are subject to viscous damping, which is neglected in the calculation but suppresses these modes in the experiments. Since only the lowest pure modes are strong enought to grow into the nonlinear regime, we restrict the calculation to perturbations of the form

$$\frac{\delta\rho}{\rho} = e^{-1/2\ \beta z} \sum_m \delta S_m(t) \cos\frac{m\pi x}{D} \cos\frac{m\pi z}{h} \tag{5.23}$$

$$\delta v_z = e^{-1/2\ \beta z} \sum_m \delta V_m(t) \cos\frac{m\pi x}{D} \cos\frac{m\pi z}{h} \tag{5.24}$$

$$\delta v_x = e^{-1/2\ \beta z} \sum_m \delta V_m(t) \frac{D}{m\pi} \sin\frac{m\pi x}{D} \left(\frac{\beta}{2}\cos\frac{m\pi z}{h} + \frac{m\pi}{h}\sin\frac{m\pi z}{h}\right) \tag{5.25}$$

The summation variable m runs in principle from 1 until ∞, but the ground mode and its lowest harmonics are dominant. For all these modes q is given by q_{max} of (5.22). In the following q denotes always this "working point" in the middle of the instability interval, and l is defined by $l = 2\ b_o/\omega^2 q$. Then (5.20) is reduced to

$$\beta\delta v_x + \frac{\partial}{\partial z}\delta v_x - \frac{\partial}{\partial x}\delta v_z = -\ \beta l \frac{\partial}{\partial x}\delta v_z \tag{5.26}$$

Now (5.17) can be integrated with respect to x by applying (5.16), and we are left with the following system of nonlinear equations for the unknown functions $\delta S_m(t)$ and $\delta V_m(t)$:

$$\left(\frac{\partial}{\partial t} + \delta\vec{v}\cdot\nabla\right) \delta v_z = -\ \frac{\gamma(t)}{\beta l} \frac{\delta\rho}{\rho} \tag{5.27}$$

$$\left(\frac{\partial}{\partial t} + \delta\vec{v}\cdot\nabla\right) \frac{\delta\rho}{\rho} = -\ \beta\ \delta v_z \tag{5.28}$$

5.2 Derivation of Nonlinear Equations for the Ground Mode and its First Harmonic

If a mode with a certain m grows or decays, the components δS_m and δV_m must grow or decay simultaneously. It is thus reasonable to assume that the relative contributions of the different modes to the expansions (5.23) for $\delta\rho/\rho$ and (5.24) for δv_z have the same amplitudes. This implies that at any time $\delta\rho/\rho$ is proportional to δv_z. The proportionality factor may still be a function of time:

$$\delta v_z\ (x,z,t) = \Psi(t) \frac{\delta\rho}{\rho}(x,z,t) \tag{5.29}$$

or $\quad \delta V_m(t) = \Psi(t)\ \delta S_m(t) \qquad$ for all m $\quad$ (5.30)

It is convenient to introduce dimensionless quantities by

$$t = \frac{2}{\omega}\tau = \frac{T}{\pi}\tau, \quad (x,z) = \frac{h}{\pi}(\xi,\zeta) \tag{5.31}$$

$$(\delta v_x, \delta v_z, \delta V_m, \Psi) = \frac{h}{T}(\delta u_x, \delta u_z, \delta U_m, \psi) \tag{5.32}$$

In addition we define δU_z and δU_x by

$$\delta u_z = \psi\,\delta U_z = \psi\,\frac{\delta\rho}{\rho} = \psi\, e^{-\beta h/2\pi\zeta} \sum_m \delta S_m(\tau) \cos\frac{mh}{D}\xi \cos m\zeta \tag{5.33}$$

$$\delta u_x = \psi\,\delta U_x = \psi\, e^{-\beta h/2\pi\,\zeta} \sum_m \delta S_m(\tau) \frac{D}{mh} \sin\frac{mh}{D}\xi \left(\frac{\beta h}{2\pi} \cos m\zeta + m \sin m\zeta\right) \tag{5.34}$$

With these notations the system (5.27, 5.28) is transformed to

$$\frac{\partial}{\partial\tau}(\psi\delta U_z) = \frac{a-2q\cos 2\tau}{\beta h/\pi}\delta U_z - \psi^2\,\mathbb{D}\delta U_z \tag{5.35}$$

$$\frac{\partial}{\partial\tau}\delta U_z = -\frac{\beta h}{\pi}\psi\,\delta U_z - \psi\,\mathbb{D}\,\delta U_z \tag{5.36}$$

where the operator $\mathbb{D}$ is defined as

$$\mathbb{D} = \delta U_x \frac{\partial}{\partial\xi} + \delta U_z \frac{\partial}{\partial\zeta} \tag{5.37}$$

and a is the Mathieu parameter $a = -q^2$ taken at the working point $q = q_{12} = q_{max} = q_o/2$. It is interesting to note that equations (5.35) and (5.36) can be combined in order to cancel the nonlinear correction terms. The resulting differential equation

$$\dot\psi = \frac{d\psi}{d\tau} = \frac{a-2q\cos 2\tau}{\beta h/\pi} + \frac{\beta h}{\pi}\psi^2 \tag{5.38}$$

is a Riccati equation for $\psi(\tau)$. Since it does not include the nonlinear terms of (5.35, 5.36), the solution ψ must have the same form as in the linear case. But in the linear case all δS_m obey to the same differential equation, i.e. Mathieu's differential equation (3.47), where χ must be the growing solution $\sim e^{\mu\tau}$ with the growth rate $\mu = \mu_{max} = \frac{1}{2}\sqrt{2}\,q$. We denote this Mathieu function by χ_{lin}, and use it in the linearized form of equation (5.36) to get an explicit solution of the Riccati equation:

$$\psi = -\frac{\pi}{\beta h}\frac{\dot{\chi}_{1in}}{\chi_{1in}} \tag{5.39}$$

The function $\psi(\tau)$ oscillates periodically about some finite mean value $\bar{\psi} \sim 1$. We now have to find the nonlinearly corrected differential equations for the components $\delta S_m(\tau)$ of δU_z. First we supplement (5.36) with a similar equation for $\delta\dot{U}_x$ by the following transformations:

$$\frac{\partial}{\partial\xi}\delta\dot{U}_z = -\frac{\beta h}{\pi}\psi\frac{\partial}{\partial\xi}\delta U_z - \psi\frac{\partial}{\partial\xi}(\delta U_x\frac{\partial}{\partial\xi} + \delta U_z\frac{\partial}{\partial\zeta})\,\delta U_z \tag{5.40}$$

Application of (5.16) in dimensionless form permits to commute $\partial/\partial\xi$ with the bracket operator $\mathbb{D}$. Then (5.26) can be used in the form

$$(1 - \beta 1)\frac{\partial}{\partial\xi}\delta\dot{U}_z = (\frac{\beta h}{\pi} + \frac{\partial}{\partial\zeta})\,\delta U_x \tag{5.41}$$

and (5.40) becomes

$$(\frac{\beta h}{\pi} + \frac{\partial}{\partial\zeta})\,\delta\dot{U}_x = -\frac{\beta h}{\pi}\psi\,(\frac{\beta h}{\pi} + \frac{\partial}{\partial\zeta})\,\delta U_x - \psi\,\mathbb{D}\,(\frac{\beta h}{\pi} + \frac{\partial}{\partial\zeta})\,\delta U_x \tag{5.42}$$

Again applying (5.16) it results a differential equation of the form $(\beta h/\pi + \partial/\partial\zeta)f = 0$. Only the trivial solution $f \equiv 0$ makes sense and is compatible with the linear case. Hence we have

$$\frac{\partial}{\partial\tau}\delta U_x = -\frac{\beta h}{\pi}\psi\,\delta U_x - \psi\mathbb{D}\delta U_x, \tag{5.43}$$

and by combination with (5.36) it follows

$$\frac{\partial}{\partial\tau}\mathbb{D} = -\frac{\beta h}{\pi}\psi\,\mathbb{D} - \psi\,\mathbb{D}^2 \tag{5.44}$$

Differentiating (5.36) with respect to time and inserting equations (5.35), (5.38) and (5.44) yields

$$\begin{aligned}\delta\ddot{U}_z &= -\frac{\beta h}{\pi}(\psi\delta U_z)^{\bullet} - \dot{\psi}\mathbb{D}\delta U_z - \psi\dot{\mathbb{D}}\delta U_z - \psi\mathbb{D}\delta\dot{U}_z \\ &= \frac{\beta h}{\pi}\,(\frac{a-2q\cos 2\tau}{\beta h/\pi}\delta U_z - \psi^2\,\mathbb{D}\,\delta U_z) - (\frac{a-2q\cos 2\tau}{\beta h/\pi} + \frac{\beta h}{\pi}\psi^2)\,\mathbb{D}\,\delta U_z \\ &\qquad + \psi\,(+\frac{\beta h}{\pi}\,\psi\mathbb{D} + \psi\mathbb{D}^2)\,\delta U_z + \psi\,\mathbb{D}\,(+\frac{\beta h}{\pi}\psi\,\delta U_z + \psi\,\mathbb{D}\,\delta U_z)\end{aligned}$$

$$\begin{aligned}\delta\ddot{U}_z &= -(a-2q\cos 2\tau)\,\delta U_z + (-\frac{a-2q\cos 2\tau}{\beta h/\pi} + \frac{2\beta h}{\pi}\psi^2)\,\mathbb{D}\delta U_z \\ &\qquad + \psi^2\,[\mathbb{D}^2\,\delta U_z + \mathbb{D}(\mathbb{D}\delta U_z)\,]\end{aligned} \tag{5.45}$$

Note that operating with $\mathbb{D}^2$ on δU_z does not give the same result as the twice repeated application of $\mathbb{D}$ on δU_z. The first term on the right hand side is already known from linear theory, the additional terms represent the nonlinear coupling between the different modes. We are interested in the fate of the pure modes which can grow into the regime of nonlinear effects. Their second derivatives appear on the left hand side of (5.45) in terms of the form $\ddot{\delta S}_m \cos \frac{mh}{D} \xi \cos m \zeta$. We must collect the terms with the same spatial dependence on the right hand side and disregard all other terms. In this way eq. (5.45) becomes a system of coupled equations for the self and mutual interactions of the δS_m.

To facilitate the evaluation, we consider only the interactions of the ground mode m=1 and its first higher harmonic m=2. Furthermore we introduce a smallness parameter ε by

$$\varepsilon = \frac{\beta h}{\pi} \qquad (\approx \frac{1}{24}) \tag{5.46}$$

and have

$$\begin{aligned} q &\sim \varepsilon \qquad (= \frac{1}{30}) \\ a &= -q^2 \sim \varepsilon^2 \end{aligned} \tag{5.47}$$

The numbers in brackets correspond to Wolf's /2/ experiment. By virtue of (5.13) we have also

$$\delta S_1 \sim \varepsilon \tag{5.48}$$

As an additional assumption we take

$$\delta S_2 << \delta S_1 \tag{5.49}$$

This will be justified afterwards. It is now an easy but somewhat lengthy matter to perform the calculations in (5.45), to expand in powers of ε and to select and collect the terms with the desired spatial dependence $\cos h/D\ \xi \cos \zeta$ or $\cos 2h/D\ \xi \cos 2\ \zeta$. E.g. one must apply many times the formulae for products of trigonometric functions. Retaining only the dominant terms results in a drastic simplification. The relevant nonlinear contributions come from the last term $\mathbb{D}(\mathbb{D}\delta U_z)$ in (5.45). Our final equations are

$$\ddot{\delta S}_1 + (a - 2q \cos 2\tau)\, \delta S_1 + \frac{1}{2} \psi^2 \, \delta S_1^3 = 0 \tag{5.50}$$

$$\ddot{\delta S}_2 + (a - 2q \cos 2\tau)\, \delta S_2 + \underbrace{2\, \psi^2 \, \delta S_1^2}_{\Delta a(\tau)} \delta S_2 = 0 \tag{5.51}$$

So we find that in the Mathieu equation for δS_1 a cubic correction is added, and the nonlinear saturation is caused by selfinteraction only.

The correction to the Mathieu equation for δS_2 means a shift of the Mathieu parameter a with a transient time dependence. The time average of $2\, \psi^2 \delta S_1^2$ is in the regime of nonlinear saturation of δS_1 of the order $a \sim \varepsilon^2$, and the superposed time modulation can be neglected in comparison with $2q \cos 2\tau$.

5.3 Solution of the Differential Equation for the Ground Mode

We next investigate the time behaviour of $\chi = \delta S_1$ in (5.50). First we need expressions for χ_{1in} and ψ in (5.39). The expansion for the exponentially growing Mathieu function is taken from /7/:

$$\chi_{1in} = e^{\mu\tau} \left[1 - \frac{q}{4} \frac{e^{2i\tau}}{1-i\mu} + \frac{q^2}{32} \frac{e^{4i\tau}}{(1-i\mu)(2-i\mu)} + \ldots + c.c. \right]$$

$$\chi_{1in} = e^{\mu\tau} \left[1 \underbrace{- \frac{q}{2} (\cos 2\tau}_{O(\varepsilon)} - \underbrace{\mu \sin 2\tau) + \frac{q^2}{32} \cos 4\tau}_{O(\varepsilon^2)} + O(\varepsilon^3) \right] \tag{5.52}$$

The time derivative is

$$\dot{\chi}_{1in} = e^{\mu\tau} \left[\mu - \mu \frac{q}{2} \cos 2\tau + \ldots \right.$$
$$\left. - \frac{q}{2} (-2 \sin 2\tau - 2\mu \cos 2\tau) - \frac{q^2}{8} \sin 4\tau + \ldots \right]$$

$$\dot{\chi}_{1in} = e^{\mu\tau} \left[\mu + \frac{q}{2} (2 \sin 2\tau + \mu \cos 2\tau) - \frac{q^2}{8} \sin 4\tau + \ldots \right] \tag{5.53}$$

In the expansion for ψ only the leading term will be required:

$$\psi = - \frac{1}{\varepsilon} \frac{\dot{\chi}_{1in}}{\chi_{1in}} = - \frac{1}{\varepsilon} (\mu + q \sin 2\tau + \ldots) \tag{5.54}$$

$$\psi^2 = \frac{1}{\varepsilon^2} \left(\mu^2 + 2\, \mu q \sin 2\tau + q^2 \frac{1-\cos 4\tau}{2} + \ldots\right)$$

$$\psi^2 = \frac{1}{\varepsilon^2} (\mu^2 + \frac{1}{2} q^2 + 2\ \mu q \sin 2\tau - \frac{1}{2} q^2 \cos 4\tau + \ldots) \tag{5.55}$$

The time average is

$$\overline{\psi^2} = \frac{1}{\varepsilon^2} (\mu^2 + \frac{1}{2} q^2) = \frac{q^2}{\varepsilon^2} \tag{5.56}$$

As a first step we replace the coefficients of χ and χ^3 in (5.50) by their time averages:

$$\ddot{\chi} + a\chi + \frac{1}{2} \overline{\psi^2}\ \chi^3 = 0 \tag{5.57}$$

This equation corresponds to the motion of a mass point in a parabolic potential well of fourth order (fig. 8):

$$\ddot{\chi} = - \frac{d}{d\chi} V(\chi) \text{ with} \tag{5.58}$$

$$V(\chi) = \frac{1}{2} a\chi^2 + \frac{1}{8} \overline{\psi^2}\ \chi^4 = - \frac{1}{2} q^2\chi^2 \quad 1 - (\frac{\chi}{2\varepsilon})^2 \tag{5.59}$$

The potential hill in the center causes the linear instability. The two potential minima correspond to the nonlinear stabilization and saturation. The symmetry reflects the fact that both orientations of rotation of the convective eddies are equally probable. We conclude that the original unstable static equilibrium $\chi = 0$ bifurcates into two neighbouring stationary flows $\chi = \chi_{stat} = \pm \sqrt{2}\ \varepsilon$.

Since the coefficients of the differential equation (5.50) are periodically modulated, the stationary flow must also be subject to periodic variations. We try an expansion of the form

$$\chi_{stat} = \chi_1 + \chi_2 \cos 2\tau + \chi_{3s} \sin 2\tau + \chi_{3c} \cos 4\tau + \ldots$$

$$\text{with} \quad \chi_\nu \sim \varepsilon^\nu, \ \nu = 1,2,3 \tag{5.60}$$

This form of χ_{stat} would be very similar to χ_{lin} (5.52). We substitute χ_{stat} for δS_1 in equation (5.50), use (5.55) and take into account terms up to third order in ε:

$$- \chi_2\, 4 \cos 2\tau - \chi_{3s}\, 4 \sin 2\tau - \chi_{3c}\, 16 \cos 4\tau$$

$$+ a\chi_1 - 2\, q \cos 2\tau\, (\chi_1 + \chi_2 \cos 2\tau)$$

$$+ \frac{1}{2\varepsilon^2}\, (\mu^2 + \frac{1}{2} q^2 + 2\, \mu q \sin 2\tau - \frac{1}{2} q^2 \cos 4\tau)\, \chi_1^3 + \ldots = 0 \qquad (5.61)$$

Replacing $\cos^2 \hat{2}\tau$ by $\frac{1}{2}(1+\cos 4\tau)$ and equating terms of the same time dependence yields

$$\chi_1 = \varepsilon \sqrt{- 2\, \frac{a + \frac{1}{2} q^2}{\mu^2 + \frac{1}{2} q^2}} = \varepsilon \qquad (5.62)$$

$$\chi_2 = - \frac{1}{2} q \chi_1 = - \frac{1}{2} q \varepsilon\ . \qquad (5.63)$$

Continuing in this way, the stationary solution of the nonlinear Mathieu equation up to third order in ε is found to be

$$\chi_{stat} = \varepsilon \left[1 \underbrace{- \frac{q}{2} (\cos 2\tau}_{O(\varepsilon)} \underbrace{- \frac{\mu}{2} \sin 2\tau) + \frac{q^2}{64} \cos 4\tau}_{O(\varepsilon^2)} + \ldots \right] \qquad (5.64)$$

The essential difference compared with χ_{1in} (5.52) is the replacement of the exponential factor $e^{\mu\tau}$ by the saturation amplitude $\varepsilon = \beta h/\pi$. The periodic modulation that is superposed on the exponentially growing linear solution persists in the nonlinearly saturated stationary case. The correction term of first order $- \frac{q}{2} \cos 2\tau$ is exactly the same as in the linear case, the correction term of second order is exactly one half of the linear one. We observe that the periodic modulation shifts the minimum of the potential (5.59), which defines the time average of the stationary amplitude, from $\sqrt{2}\varepsilon$ to ε. This has been indicated in fig. 8.

We can interpolate by a transient time function, which behaves for $\tau \to -\infty$ as the linear solution and for $\tau \to +\infty$ as the stationary solution, and describes the transition from growth to saturation by

$$\chi_{tran} = \varepsilon e^{\mu\tau} \left[\frac{1 - \frac{1}{2} q \cos 2\tau}{1 + e^{\mu\tau}} + \frac{\frac{1}{2} q\mu \sin 2\tau + \frac{1}{32} q^2 \cos 4\tau}{1 + 2\, e^{\mu\tau}} + \ldots \right] \qquad (5.65)$$

According to this evolution function, at time $\tau = 0$ half of the final amplitude ε is reached. If the ground mode δS_1 has grown up to this level, we can see from (5.51) that then the first harmonic δS_2 will be superseded by δS_1. The effective Mathieu parameter becomes

$$a_{eff} = a + \Delta a(0) = a + 2\,\overline{\psi^2}\,\overline{\delta S_1^2}(0) = a + 2\,\frac{q^2}{\varepsilon^2}\,\frac{\varepsilon^2}{4}$$

$$= a + \frac{1}{2}q^2 = -\frac{1}{2}q^2 = a_o(q) \qquad (5.66)$$

Hence a_{eff} lies exactly on the stability boundary $a_o(q)$ in the Mathieu chart, so that the growth of the m = 2 mode is completely suppressed by the nonlinear coupling with the m = 1 mode, and a complete stabilization is achieved. Thus nonlinear dynamics implies in the present case that the

larger mode swallows the smaller one. This justifies a posteriori the assumption (5.49) that δS_2 should remain much smaller than δS_1. It explains also the pronounced dominance of the ground mode in the experiment. Nevertheless, it may happen incidentally that the m = 2 mode is much more strongly excited from the beginning than the ground mode. Then the mode m = 2 may prevail temporarily, and become visible experimentally. In fact this was the case in one out of numerous experiments of Hopmann et al. /3/. It took some seconds until finally m = 2 was again superseded by m = 1.

5.4 Calculation of Mean Convective and Parametric Mass Transport

First we must have the amplitude δU_1 of the velocity of the ground mode in leading order:

$$\delta U_1 = \psi\delta S_1 = \psi\chi_{stat} = -\frac{1}{\varepsilon}(\mu + q\sin 2\tau + \ldots)\,\varepsilon(1 - \ldots)$$

$$\delta U_1 = -(\mu + q\sin 2\tau) + O(\varepsilon^2) \qquad (5.67)$$

In dimensional form this becomes

$$\delta V_1 = -\frac{h}{T}(\mu + q\sin\ \omega t) = -\frac{\omega hq}{2\pi}\left(\frac{1}{2}\sqrt{2} + \sin\ \omega t\right) \qquad (5.68)$$

We see that the velocity amplitude oscillates considerably, the amplitude of the time variation being even larger than the time average. The experiment, however, gives the impression of a steady vortex motion of the fluid, and the superposed oscillations with the applied shake frequency ω are not observed. The reason is the diagnostic technique which must compensate for the oscillatory movement of the vessel by application of the stroboscopic effect, i.e. one flashes at the vessel with exactly the same frequency ω (or ω/n, $n = 2, 3, \ldots$) used for shaking, so that a sequence of photographs or videographs is produced taken always at equal phases of the movement. Thus a fluid motion with constant velocity is simulated. Of course the convective mass transport is determined only by this time average of the velocity. For the density and the vertical velocity we have the representations

$$\left.\begin{matrix} \frac{\delta\rho}{\rho} \\ \delta v_z \end{matrix}\right\} = e^{-1/2\,\beta z} \left\{\begin{matrix} \delta S_1(t) \\ \\ \delta V_1(t) \end{matrix}\right\} \cos\frac{\pi x}{D}\cos\frac{\pi z}{h} \tag{5.69}$$

$$0 \leq x \leq D, \quad 0 \leq z \leq h$$

The mass flow is given by the convective mass current density, that is the vertical mass transport per time unit across the area unit:

$$j_{con} = \frac{1}{D}\int_0^D \delta\rho\ \delta v_z\ dx \tag{5.70}$$

$$= \frac{1}{D}\,\rho(z)\ e^{-\beta z}\ \delta S_1\ \delta V_1\ \cos^2\frac{\pi z}{h}\int_0^D \cos^2\frac{\pi x}{D}\,dx$$

$$j_{con} = \frac{1}{2}\,\rho_o\ \delta S_1\ \delta V_1\ \cos^2\frac{\pi z}{h} \tag{5.71}$$

and the time average is

$$\overline{j_{con}} = -\frac{1}{2}\,\rho_o\ \varepsilon\ \frac{\omega h q}{4\ \pi}\,\sqrt{2}\,\cos^2\frac{\pi z}{h} \tag{5.72}$$

With $\varepsilon = \beta h/\pi = \frac{\rho_o'}{\rho_o}\frac{h}{\pi}$ the result is

$$\overline{j_{con}} = -\mathcal{D}\ \rho_o'\ \cos^2\frac{\pi z}{h} \tag{5.73}$$

where the diffusion coefficient is given by

$$\mathcal{D} = \frac{\sqrt{2}}{8\pi^2}\,q\omega h^2 = \frac{\sqrt{2}}{2\pi}\quad\frac{g}{b_o}\,\frac{h^2}{T} \tag{5.74}$$

The sign of $\overline{j_{con}}$ indicates that the transport is directed downwards. We have thus calculated a diffusion coefficient $\mathcal{D}$ which gives an upper bound for the convective mass transport across the dynamically stabilized diffuse boundary layer, because the considered quasistationary sheet detachment is certainly more effective than any periodically intermittent sheet detachment.

The mass current density (5.73) depends on z and therefore causes a non-linear steepening of the density profile near the midplane $z = h/2$.
We call this density change $\delta^2\rho(z,t)$ and find from (5.36) in leading order

$$\frac{\partial}{\partial\tau}\frac{\delta^2\rho}{\rho} = -\psi\mathcal{D}\ \delta U_z \tag{5.75}$$

$$= \psi e^{-\varepsilon\zeta}\frac{1}{2}\ \delta S_1^2 \sin 2\zeta = e^{-\varepsilon\zeta}\frac{1}{2}\ \delta U_1\ \delta S_1 \sin 2\zeta$$

or in dimensional form

$$\frac{\partial}{\partial t}\ \delta^2\rho = \rho_o \frac{\pi}{2h}\ \delta V_1 \delta S_1 \sin\frac{2\pi z}{h} \tag{5.76}$$

Comparison with (5.71) shows, that the continuity equation

$$\frac{\partial}{\partial t}\ \delta^2\rho + \frac{\partial}{\partial z}\ j_{con} = 0 \tag{5.77}$$

is fulfilled. We write $\delta^2\rho$ in the form

$$\delta^2\rho = -\rho_o\delta^2 S_1(t) \sin\frac{2\pi z}{h} = \rho_o \int_{-\infty}^{t} \frac{\pi}{2h}\ \delta V_1 \delta S_1 dt \sin\frac{2\pi z}{h} \tag{5.78}$$

and look at the total density gradient

$$\frac{\partial}{\partial z}\ (\rho+\delta^2\rho) = \rho' - \rho_o\ \delta^2 S_1 \frac{2\pi}{h} \cos\frac{2\pi z}{h} \tag{5.79}$$

$$= \rho' - \rho_o\ \delta^2 S_1 \frac{2\beta}{\varepsilon}\left(1 - 2\sin^2\frac{\pi z}{h}\right)$$

$$\overline{\frac{\partial}{\partial z}(\rho+\delta^2\rho)} = \underbrace{\rho' - \rho_o' \frac{2\overline{\delta^2 S_1}}{\varepsilon}}_{\rho'_{par}} + \rho_o' \frac{\overline{4\delta^2 S_1}}{\varepsilon} \sin^2\frac{\pi z}{h} \tag{5.80}$$

The bar denotes again averaging, i.e. suppression of the superposed oscillations. If the $\sin^2 \pi z/h$-term represents the deviation from the threshold value ρ'_{par} for the excitation of parametric instabilities, and if for simplicity the parametrically induced $\overline{\text{diffusion}}$ is assumed to be proportional to this deviation, one can choose $\overline{\delta^2 S_1}$ such that the associate mass current density is given by

$$\overline{j_{par}} = -\mathcal{D}\, \rho'_o \sin^2 \frac{\rho z}{h} \tag{5.81}$$

This removes the z-dependence of the total mass current density:

$$\overline{j_{tot}} = \overline{j_{con}} + \overline{j_{par}} = -\mathcal{D}\, \rho'_o = \text{constant} \tag{5.82}$$

We thus arrive at a stationary diffusive mass flow where the nonlinear steepening of the density gradient by convective cells is everywhere balanced by a counteracting parametric flattening. We can say that the mass transport when passing across the boundary layer must "change horses" twice. The dominating process is convective near the limiting surfaces and parametric near the midplane. This is schematically illustrated by fig. 9. The nonlinear correction $\delta^2\rho(z)$ of the initial density profile $\rho(z)$ has been much exaggerated. Since we know from linear theory that the parametric resonances $\overline{\text{have}}$ very large growth rates (see fig. 5), we need only a very small $\overline{\delta^2 S_1}$ to produce the necessary diffusion coefficient $\mathcal{D}$ for preventing a further steepening of the density profile. This keeps the nonlinear deformation of the initial density profile $\rho(z)$ and the difference between $\rho'(z)$ and $\rho'_{par}(z)$ so small that it can be neglected. The real stationary $\delta^2\rho(z)$ could not be discerned in fig. 9. For this reason we can dispense with the assumption that the parametric diffusion is proportional to the deviation from the threshold gradient ρ'_{par}. It is sufficient to have a monotonic increase. Then the density profile can be automatically adjusted such as to maintain a stationary z-independent mass flow. $\delta^2\rho(z)$ will then behave different from $\sin 2\pi z/h$, but again it will be negligibly small. Hence we need not care about the details of the parametric diffusion, all we must know is that it exists and that it is strong enough. We conclude therefore that the stationary mass transport is determined exclusively by the nonlinear saturation of the convective cells, that is by the diffusion coefficient $\mathcal{D}$ (5.74). We have not considered the continuation of mass transport into the regions of homogeneous density above and below the boundary layer, but it is known from linear theory that the vortex motion of the convective cells reaches far into these regions and, with the assistance of gravity respectively buoyancy, should provide the required mass motion and density mixing. This is confirmed by experimental evidence.

For purposes of illustration we choose an example with numbers similar to Wolf's /2/ experiment:

$$\rho_o = \tilde{\rho}_1 = 1.4 \frac{g}{cm^3}, \ \tilde{\rho}_2 = \tilde{\rho}_1 \ e^{\beta h} = 1.6 \frac{g}{cm^3}$$

$$D = 0.78 \text{ cm}, \ q = \frac{2}{b_o} g = \frac{1}{30}, \ g = 981 \frac{cm}{sec^2}$$

$$\beta h = \ln \frac{\tilde{\rho}_2}{\tilde{\rho}_1} = \ln \frac{8}{7} = 0.1335$$

From (5.1) follows $\quad q_{par} = 0.934$

From (5.3) and (5.4) follows

$$\frac{D^2 + h^2}{h^2} = \frac{b_o}{2g} q_{par}$$

$$h = \frac{D}{\sqrt{\frac{b_o}{2g} q_{par} - 1}} = 0.1501 \text{ cm}$$

From (5.4) follows further

$$\omega = \sqrt{\frac{2 \ b_o \beta}{q_{par}}} = \sqrt{\frac{4g}{h} \frac{b_o}{2g} \frac{\beta h}{q_{par}}} = 334.8 \text{ sec}^{-1}$$

$$\frac{1}{T} = \frac{\omega}{2\pi} = 53.29 \text{ Hz}$$

Hence we must shake with 53 Hz instead of 100 Hz to satisfy the conditions for quasistationary convection. The diffusion coefficient is according to (5.74)

$$\mathcal{D} = \frac{\sqrt{2}}{4\pi} \frac{2g}{b_o} \frac{h^2}{T} = 4.504 \times 10^{-3} \frac{cm^2}{sec}$$

and the associate mass current density is according to (5.82)

$$\bar{j} = -\mathcal{D}\,\rho_o' = -\mathcal{D}\,\tilde{\rho}_1\,\frac{\beta h}{h} = -\,5.608 \times 10^{-3}\,\frac{g}{cm^2\ sec}$$

$$\bar{j} \approx -5.6\,\frac{mg}{cm^2\ sec}$$

This can be compared with the transport by periodically intermittent sheet detachment. The mass transport ΔM per period ΔT is given by about the hatched area in fig. 7b, that is

$$\Delta M = \frac{1}{2}\;\frac{\tilde{\rho}_2 - \tilde{\rho}_1}{2}\;\frac{h_{par}}{2} \approx 5\;\frac{mg}{cm^2}$$

The experimental period length was of the order of 10 sec, so that

$$\bar{j} = -\,\frac{\Delta M}{\Delta T} \approx -\,0.5\,\frac{mg}{cm^2 sec} \tag{5.84}$$

We see from (5.83) and (5.84) that the quasistationary diffusion can be an order of magnitude higher than the intermittent diffusion. While the latter is determined mainly by the long quiescent phases with a slow micro-turbulent diffusion similar to ordinary diffusion, the former is purely convective with an induced parametric activity and defines an upper bound for the possible anomalous transport.

6. Diffusion by Convective Cells in Magnetized High Temperature Plasmas

So far we have considered the diffusion by convective cells in dynamically stabilized liquid boundary layers. The long wave Rayleigh-Taylor instabilities cannot be fully suppressed, but they are nonlinearly saturated and produce an anomalously increased transport by convective cells of a definite wave length. In the magnetically confined high temperature plasma of a nuclear fusion machine, e.g. a tokamak, there are also Rayleigh-Taylor instabilities. They are usually called interchange modes (e.g. flute modes, ballooning modes), and arise in magnetic fields with lines of convex curvature, so that centrifugal force and density gradient are in opposite directions. The centrifugal force acts as a fictitious gravity force and creates together with the plasma inhomogeneity a weak but finite source of free energy. We shall see that there exists probably a slowly growing mode with a relatively long wave length that is most dangerous in the sense that is possesses the largest growth rate. Saturation occurs when this most unstable mode is nonlinearly stabilized so that it becomes marginally stable. Then, however, all other long wave length modes are stable, and this entails that the $\vec{k}$-spectrum at saturation must have a sharp peak. The associated mass flow exhibits again the pattern of convective cells. Note that this does not alter the configuration as a whole, and the plasma equilibrium is stably maintained. The role of the parametric resonances of the hydrodynamic model can be taken in the plasma e.g. by the drift instabilities which occupy part of the shorter wave length region of the $\vec{k}$-spectrum.

Since the understanding of anomalous plasma transport is a central problem of nuclear fusion and since the convective cells are a major candidate for the explanation of anomalous transport, one is tempted to try a new approach to this problem by transferring the theory of nonlinear saturation of convective cells from the liquid to the plasma. We will first summarize some characteristic features of the Rayleigh-Taylor and drift instabilities in plasmas, and then set up a simple plasma model allowing to work out the analogies to the hydrodynamic model and to estimate the maximum possible anomalous plasma transport.

6.1 Some Basic Features of Rayleigh-Taylor and Drift Instabilities

6.1.1 Interchange Modes and Localized Convective Cells

Electrons and Ions moving with thermal velocities along magnetic field lines of curvature radius R experience a centrifugal force

$$K = \frac{m_e v_{Te}^2 + m_i v_{Ti}^2}{R} = \frac{kT_e + kT_i}{R} \tag{6.1}$$

and hence an effective centrifugal acceleration

$$g = \frac{kT_e + kT_i}{(m_e + m_i)R} \approx \left(1 + \frac{T_e}{T_i}\right) \frac{v_{Ti}^2}{R} \gtrsim \frac{v_s^2}{R} \tag{6.2}$$

$$\text{with} \quad v_s = \sqrt{\frac{kT_e}{m_i}} = \text{ion sound velocity} \tag{6.3}$$

We assume that the acceleration is directed "outwards", i.e. in the direction of decreasing density, so that the plasma is Rayleigh-Taylor unstable. The role of the dynamic stabilization is taken in the plasma by the magnetic field that forces electrons and ions to gyrate on circular orbits around the field lines. In combination with pressure gradients and "gravity" g this leads to particle drifts

$$\vec{v}_D = \frac{\vec{f} \times \vec{B}}{qB^2} = \frac{\left(-\frac{1}{n} \nabla p + m\vec{g}\right) \times \vec{B}}{qB^2} \tag{6.4}$$

Neglecting temperature gradients the drift velocity is

$$\vec{v}_D = \frac{\left(-\frac{kT}{m} \nabla \ln n + \vec{g}\right) \times \vec{B}}{\Omega_B B} \tag{6.5}$$

Diamagnetic drifts and gravitational drifts must be considered for ions and electrons separately. For ions we have

$$v_{*i} = \frac{v_{Ti}^2}{\Omega_i} \kappa = \frac{kT_i}{q_i B} \kappa = \frac{kT_i}{q_i B} \left|\frac{\nabla n}{n}\right| \tag{6.6}$$

$$v_{Gi} = \frac{g}{\Omega_i} \gtrsim \frac{v_S^2}{\Omega_i R} \tag{6.7}$$

κ is a reciprocal scale length for the density increase (which was called β in the hydrodynamic model), and $\Omega_i = \Omega_{Bi} = q_i B/m_i$ is the ion gyrofrequency. For electrons i is replaced by e. The ion gyro radius $r_i = v_{Ti}/\Omega_i$ is much greater than the electron gyro radius $r_e = v_{Te}/|\Omega_e|$ (provided that T_e is not very much greater than T_i, which we suppose). Therefore for the stabilization of the Rayleigh-Taylor instability only the ion gyro-motion is relevant. Ω_i replaces the shake frequency of the hydrodynamic model, r_i the amplitude of the oscillatory motion. Ω_i and r_i in turn depend on the plasma parameters magnetic field strength B and temperature $T_i \lesssim T_e$.

An analysis based on the kinetic theory (see e.g. Mikhailovskii /8/ and /9/) leads to the following dispersion relation for the flute mode:

$$\omega^2 - \omega k_x v_{Di} - k_{||}^2 v_A^2 + \frac{k_x^2}{k_\perp^2} g \kappa = 0 \tag{6.8}$$

$$\omega = \frac{1}{2} k_x v_{Di} \pm \sqrt{\frac{1}{4} k_x^2 v_{Di}^2 + k_{||}^2 v_A^2 - \frac{k_x^2}{k_\perp^2} g\kappa} \tag{6.9}$$

where we have used

$$\vec{g} = - g \vec{e}_y, \ \vec{B} = B \vec{e}_z, \ \vec{e}_x = \vec{e}_y \times \vec{e}_z \tag{6.10}$$

$$k_{||}^2 = k_z^2 , \quad k_\perp^2 = k_x^2 + k_y^2 \tag{6.11}$$

$$v_A = \sqrt{\frac{B^2}{\mu_o \rho}} = \text{Alfvén velocity} \tag{6.12}$$

We have rotated the coordinate system relative to the hydrodynamic model so that the magnetic field points into the z - direction. The last term under the root of (6.9) is destabilizing and describes the Rayleigh-Taylor instability. The first term is stabilizing and describes the influence of the finite ion gyro radius. The second term is also stabilizing and describes the bending of field lines by finite $k_{||}$. For vanishing $k_{||}$ we have pure flute modes which have the fastest growth. In a magnetically confined plasma, however, the shearfree case is the exception, in general the field lines are sheared. Hence $k_{||}$ is a function of y, and near $k_{||} = 0$ we have $k_{||} = \chi k_x y$, where χ is a reciprocal scale length as measure for the shear, and y = 0 has been chosen for $k_{||} = 0$. We conclude that the Rayleigh-Taylor instability is localized in a neighbourhood of y = 0, at larger distances the flute modes are damped away and thus cannot exist. The range of existence $|y| \lesssim \Delta y$ can be estimated as follows

$$k_{||} v_A \lesssim \sqrt{g\kappa} \tag{6.13}$$

$$k_{||}\sqrt{\frac{B^2}{\mu_o \rho}} \lesssim \sqrt{\frac{v_s^2}{R}\kappa} \sim \sqrt{\frac{p}{\rho}\frac{\kappa}{R}}$$

$$k_{||} = \chi k_x \Delta y \lesssim \sqrt{\beta \frac{\kappa}{R}} \tag{6.14}$$

The plasma β is a small number, whereas κ should be much greater than $\frac{1}{R}$. We take $\beta\kappa$ to be of the order of $\frac{1}{R}$. Furthermore we put $\Delta y \sim 1/k_y$, because the maximum admissible Δy corresponds to a minimum possible k_y. Then it follows from (6.14), that for instability the wave numbers must satisfy

$$\frac{k_y}{k_x} \gtrsim \chi R .$$

On the other hand the Rayleigh-Taylor instability grows only for large $g\kappa k_x^2/k_\perp^2 = g\kappa/(1 + k_y^2/k_x^2)$. Hence we should have $k_y/k_x \lesssim 1$. We thus find optimal conditions for growth, if the shear is small enough and if both wavenumbers are of equal order:

$$\chi R \lesssim 1 \text{ and } \frac{k_y}{k_x} \sim 1 \tag{6.15}$$

Up to now we only have a restriction on the ratio of the wave numbers, not on their magnitudes. But we must also compare the stabilizing gyro term with $g\kappa$:

$$k_x v_{Di} \sim k_x v_{*i} \lesssim \sqrt{g\kappa} \tag{6.16}$$

$$k_x r_i v_{Ti} \kappa \lesssim v_s \sqrt{\frac{\kappa}{R}}$$

$$k_x^2\, r_i^2 \lesssim \frac{T_e}{T_i \kappa R} \sim \frac{v_{Gi}}{v_{*i}} << 1 \tag{6.17}$$

This holds if T_e is not much greater than T_i. We thus find that only wavelengths much larger than the ion gyro radius can contribute to instability. The wavelengths, however, cannot be arbitrarily large. They are limited by the geometry and dimensions of the plasma. The theory that results in formula (6.9) supposes an idealized plane geometry. If the wave length is so large that deviations from plane geometry become appreciable over one wave length, a severe deterioration of the undisturbed mode growth is to be expected. Therefore, in tokamaks, the wavelength must be small against the minor radius of the plasma ring. In our calculations we will assume that the wave length is small against the scale length of the density gradient, $1/k_x << 1/\kappa$, which amounts to about the same condition if this scale length is of the order of the minor torus radius. Toroidal effects stemming from the major torus radius are unlikely under the indicated conditions, with the exception of course of the fictitious gravity force. Generally we can state that the vessel of the hydrodynamic model has in the plasma an equivalent in the structure of the magnetic field. For wave lengths for which the deviations from the homogeneous magnetic field become essential, convective cells can no longer exist. We infer that there is some quite narrow wave length region where Rayleigh-Taylor instabilities can grow, one wavelength will be distinguished among all others. Higher harmonics are in any case heavily damped by gyroviscosity. Thus, compared with the hydrodynamic model, in the plasma the dominance of the ground mode over the higher modes is even stronger.

The boundary layer thickness h of the hydrodynamic model must now be replaced by the width of the localization interval 2 Δy, the middle plane of the boundary layer corresponding to the singular surface $k_{||} = 0$ in the middle of the localization interval. Here the structure of the magnetic field is effective via the shear. The formation of counterrotating vortex pairs at both sides of the singular surface should in the plasma occur very much like in its hydrodynamic analogon. We only must introduce in the x-direction periodic boundary conditions instead of the fixed vessel walls, so that a whole chain of linked vortex pairs can arise. These comply with symmetry requirements, allow the conservation of the total angular momentum (in equilibrium the vorticity was zero everywhere) and produce a steepening of the density gradient at the singular surface which can be compensated by a suitable flattening mechanism to be discussed below.
In the calculation we will for simplicity assume a well defined localization interval and proceed as if the shear damping would begin suddenly at a definite distance from the singular surface, i.e. at the edges of the localization interval, whereas in reality there is a smooth transition with increasing distance. This does not change the physics, but permits the use (as in the hydrodynamic model) of trigonometric functions inside the interval and of exponentially decreasing functions outside.

There is only one peculiar or strange circumstance. The convective cells in the plasma seem to travel in the x-direction. According to (6.9) perturbations have a real part of the frequency and behave as

$$e^{i(\vec{k}\cdot\vec{r}-\omega t)} = e^{ik_x x+ik_y y-i\left(\frac{1}{2}k_x v_{Di}+i\sigma\right)t}$$

$$= e^{\sigma t}\, e^{ik_x\left(x-\frac{1}{2}v_{Di}t\right)+ik_y y} \qquad (6.18)$$

In the growth rate σ we ignore the influence of the Alfvên term that is related to localization. In addition, because of $v_{Gi} \ll v_{*i}$, we identify the total drift v_{Di} with the diamagnetic drift v_{*i}. Then

$$\sigma = \sqrt{-\frac{1}{4}k_x^2 v_{*i}^2 + \frac{k_x^2}{k_\perp^2} g\kappa} \qquad (6.19)$$

The wave numbers k_x, k_y may have either sign, disturbances with equal amplitude and opposite k_x, k_y are superposed to convective cells. According to (6.18) these would during their growth and probably also after nonlinear saturation travel with half the ion drift velocity in x-direction, in a tokamak around the small circumference. For the moment this must remain an open question.

6.1.2 Drift Modes and Locally Induced Microturbulence

A nonlinear saturation and stationary maintenance of the convective cells requires something equivalent to the parametric resonances of the liquid model. These modes of very short wave lengths were able to cancel any steepening of the density profile. In the plasma we find a corresponding phenomenon in the drift instabilities. They occur in the presence of a sufficiently large density gradient perpendicular to the magnetic field and grow fast for short waves with $k_x^2 r_i^2 \sim 1$, which coincides with stability of the flute modes. The "universal" instability of the drift waves is caused by an interaction of the electrons with the wave. For $\omega/k_{||} \sim v_{Te}$ inverse electron Landau damping may arise, i.e. the electrons give energy to the wave. An analysis based on the kinetic theory (see e.g. Similon /10/ or again Mikhailovski /8,9/) leads to the following dispersion relation for the drift mode:

$$\frac{1}{T_e}\left(1+\frac{\omega-\omega_{*e}}{\omega}\,\xi_e Z(\xi_e)\right)+\frac{1}{T_i}\left(1+\frac{\omega-\omega_{*i}}{\omega}\,\Gamma_i\xi_i Z(\xi_i)\right)=0 \tag{6.20}$$

with

$$\omega_{*e}=k_x v_{*e},\quad \omega_{*i}=k_x v_{*i}=-\frac{T_i}{T_e}\,\omega_{*e} \tag{6.21}$$

$$\xi_e=\frac{\omega}{\sqrt{2}\,v_{Te}|k_{||}|},\qquad \xi_i=\frac{\omega}{\sqrt{2}\,v_{Ti}|k_{||}|} \tag{6.22}$$

$$\Gamma_i=I_o\,(k_\perp^2 r_i^2)\,e^{-k_\perp^2 r_i^2} \tag{6.23}$$

The finite ion gyro radius gives rise to a $\Gamma_i \neq 1$. I_o is the modified Bessel function of zero order, $Z(\xi)$ is the plasma dispersion function. For

$$v_{Ti} \ll \frac{\omega}{|k_{||}|} \ll v_{Te}\quad\text{or}\quad \xi_e \ll 1 \ll \xi_i \tag{6.24}$$

we can give an approximate evaluation of (6.20):

$$\xi_e Z(\xi_e)\approx i\sqrt{\pi}\,\xi_e\,,\qquad \xi_i Z(\xi_i)\approx -1-\frac{1}{2\xi_i^2} \tag{6.25}$$

$$1+\frac{\omega-\omega_{*e}}{\omega}\,i\sqrt{\pi}\,\xi_e+\frac{T_e}{T_i}\left(1-\frac{\omega-\omega_{*i}}{\omega}\,\Gamma_i\right)=0$$

$$1-\Gamma_i+\frac{\omega-\omega_{*e}}{\omega}\,i\sqrt{\pi}\,\xi_i+\frac{T_e}{T_i}(1-\Gamma_i)+\Gamma_i+\frac{T_e}{T_i}\frac{\omega_{*i}}{\omega}\,\Gamma_i=0$$

$$\frac{T_i+T_e}{T_i}(1-\Gamma_i)+\frac{\omega-\omega_{*e}}{\omega}\left(\Gamma_i+i\sqrt{\pi}\,\xi_i\right)=0$$

$$\frac{\omega_{*e}}{\omega}=1+\frac{(1-\Gamma_i)\dfrac{T_i+T_e}{T_i}}{\Gamma_i+i\sqrt{\pi}\xi_e}\approx 1+\frac{1-\Gamma_i}{\Gamma_i}\,\frac{T_i+T_e}{T_i}\left(1-i\sqrt{\pi}\,\frac{\xi e}{\Gamma_i}\right) \tag{6.26}$$

$$\text{with}\quad \xi_e=\frac{\omega}{\omega_{*e}}\,\frac{\omega_{*e}}{\sqrt{2}\,v_{Te}|k_{||}|}\approx\frac{1}{1+\dfrac{1-\Gamma_i}{\Gamma_i}\,\dfrac{T_i+T_e}{T_i}}\,\frac{\omega_{*e}}{\sqrt{2}\,v_{Te}|k_{||}|} \tag{6.27}$$

Inserting (6.27) in (6.26) yields

$$\frac{\omega}{\omega_{*e}}=\frac{1}{1+\dfrac{1-\Gamma_i}{\Gamma_i}\,\dfrac{T_i+T_e}{T_i}-i\sqrt{\pi}\xi_e\,\dfrac{1-\Gamma_i}{\Gamma_i^2}\,\dfrac{T_i+T_e}{T_i}}$$

$$\approx \frac{1}{1+\frac{1-\Gamma_i}{\Gamma_i}\frac{T_i+T_e}{T_i}}\left[1+i\sqrt{\pi}\;\frac{\omega_{*e}}{\sqrt{2}\;v_{Te}\;|k_{||}|}\;\frac{\frac{1-\Gamma_i}{\Gamma_i^2}\;\frac{T_i+T_e}{T_i}}{(1+\frac{1-\Gamma_i}{\Gamma_i}\;\frac{T_i+T_e}{T_i})^2}\right]$$

$$\omega \approx \frac{\omega_{*e}}{1+\frac{1-\Gamma_i}{\Gamma_i}\frac{T_i+T_e}{T_i}}\left[1+i\sqrt{\pi}\;\frac{\omega_{*e}}{\sqrt{2}v_{Te}|k_{||}|}\;\frac{(1-\Gamma_i)\;\frac{T_i+T_e}{T_i}}{(1+(1-\Gamma_i)\;\frac{T_e}{T_i})^2}\right] \tag{6.28}$$

For $k_\perp^2 r_i^2 << 1$ this simplifies to

$$\omega \approx \frac{\omega_{*e}}{1+k_\perp^2 r_i^2\;\frac{T_i+T_e}{T_i}}\left[1+i\sqrt{\pi}\;\frac{\omega_{*e}}{\sqrt{2}\;v_{Te}|k_{||}|}\;\frac{k_\perp^2 r_i^2\;\frac{T_i+T_e}{T_i}}{(1+k_\perp^2 r_i^2\;\frac{T_e}{T_i})^2}\right] \tag{6.29}$$

The growth rate $\sigma = \mathrm{Im}\omega$ is obviously always positive independent of the sign of ω_{*e}. The largest growth rates occur for $\omega/|k_{||}| \sim v_{Te}$ and for $k_\perp^2 r_i^2 \sim 1$, but then the range of validity of the formulas (6.28, 6.29) is exceeded. A numerical evaluation of the dispersion relation (6.20) by Kadomtsev and Timofeev /11/ shows for $k_\perp^2 r_i^2 \gtrsim 1$ almost independent of $k_\perp^2 r_i^2$ a stability boundary with the following condition for instability:

$$|k_{||}| \lesssim 0.16\;\kappa \tag{6.30}$$

This holds if m_i is taken to be the mass of hydrogen ions. For larger $|k_{||}|$ the universal instability vanishes because of ion Landau damping. For given $|k_{||}|$ drift turbulence can arise only beyond a certain threshold value of κ. The magnitude of the $|k_{||}|$ with the maximum growth rate can be estimated as

$$|k_{||}| \sim \frac{\omega_{*e}}{v_{Te}} = k_x r_e \kappa \lesssim k_\perp r_i\;\frac{r_e}{r_i}\;\kappa \sim \frac{1}{43}\sqrt{\frac{T_e}{T_i}}\;\kappa \tag{6.31}$$

The $k_{||}$-values in (6.30) and (6.31) are comparable to the admissible $k_{||}$-values for flute modes $k_{||} \lesssim \sqrt{\beta\;\kappa/R} \sim 1/R$ according to (6.14) and (6.15). But since for drift modes the wave number k_x is much larger, namely $k_x^2 r_i^2 \sim 1$ instead of $k_x^2 r_i^2 << 1$ as for flute modes, the existence interval in the neighbourhood of y = 0 is much smaller. Thus, close to the singular surface just where the flute modes steepen the density profile, short wave drift instabilities can occur and provide, similar to the parametric resonances of the hydrodynamic model, a counteracting flattening until finally a certain stationary κ is achieved. For larger κ, the existence interval of the drift instabilities as well as the growth rate become larger $\sim \kappa$, whereas the flute modes grow only $\sim \sqrt{\kappa}$. Thus in general the stationary κ will be larger than the initial κ, and again some kind of stairs structure must be formed. If the nonlinearly saturated Rayleigh-Taylor instability causes a transport such that it can be exactly compensated by drift turbulence, the maximum possible transport is produced. Our theory is intended to yield this upper bound.

Recent theories for the nonlinear evolution of drift instabilities make the analogy to the hydrodynamic model even closer and more apparent. From (6.29) the real part of the drift ω is approximately

$$\mathrm{Re}\,\omega = \frac{k_x v_{*e}}{1 + (k_x^2+k_y^2)\, r_i^2 \, \frac{T_i+T_e}{T_i}} \tag{6.32}$$

This function has with respect to $k_x r_i$ a maximum in the neighbourhood of $k_x r_i = 1$. Therefore drift waves ("low" frequency modes) with equal $k_{||}$ and equal ω but different k_x and k_y may undergo a parametric coupling. The result of this nonlinear interaction by mode coupling is the formation of convective cells with vanishing $k_{||}$ and vanishing ω ("zero" frequency modes). Being created in the small localization interval of the drift instabilities, the convective cells should be small enough to flatten locally the density profile and to experience strong gyroviscous damping. In this way the parametric coupling takes the role of the parametric resonances. The nonlinear interaction of drift waves has been investigated e.g. by Hasegawa-Mima /12/ and Similon /10/, where many further references are listed. The essential difference of our concept is, that we take the source of the turbulence to be the formation of relatively large-scale convective cells by Rayleigh-Taylor instability (one special wave length being favoured among all others), the energy of which is via the coupling to drift instabilities finally dissipated by small-scale convective cells acting as a sink. The details of the dissipation mechanism (e.g. collisional viscosity, resonance damping) are not important, but it must be sufficiently strong. Essentially there is one long wave mode competing with many short wave modes. The energy cascading process in the wave number spectrum is directed from long to short waves. It is interesting that the theories of Hasegawa-Mima /12/ and Hasselberg-Rogister /13/ also rely on such a wave number spectrum.

In addition to the nonlinear coupling of drift waves there is still another attractive possibility for the production of small convective cells, namely the appearance of socalled modulational instabilities. If the amplitude of the drift wave is finite, the various drift velocities must be supplemented by the socalled nonlinear polarization drift that is given by

$$v_{Pi} = \frac{v_s^2}{\Omega_i} \frac{e^2}{k^2 T_e T_i} (1 - \Gamma_i) \frac{\partial}{\partial y} \left| \psi_{\vec{k}} (x,y,t) \right|^2 \qquad (6.33)$$

where $\psi_{\vec{k}}$ is the electrostatic potential of the drift wave with wave number $\vec{k}$. If the amplitude of the drift wave is slightly modulated in the x-direction, then the nonlinear polarization drift has a finite divergence, so that space charges arise and hence $\vec{E} \times \vec{B}$-drifts producing convective cells. This has been described in detail by Mima and Lee /14/. Further information and literature references can be found e.g. from Hafiz-Ur-Rahman /15/. The density profile treated by Mima and Lee avoids discontinuities. Two regions with constant but different density are connected not by a linear or exponential density profile (with unsteady derivative at the edges of the transition interval), but the density transition is supposed to follow a steady function like e.g. the hyperbolic tangent with a maximum of the derivative at y = 0. There the amplitude of the drift wave can grow beyond a certain threshold value and generate the modulational instability. The ensuing short wave convective cells flatten the density profile at y = 0 where it is the steepest, quite similar to the parametric resonances in the hydrodynamic model.

We have indicated several candidates for small-scale modes that can take the role of the parametric resonances. Probably there are still further possibilities so that we may be confident that at least one suitable mechanism is present.

6.2 Twodimensional Two-Fluid Model for Nonlinear Rayleigh-Taylor Instabilities in a Magnetized Plasma

We start from the macroscopic equations of motion and the continuity equations in the socalled drift approximation for ions and electrons:

$$\frac{d_i}{dt}\vec{v}_i = (\frac{\partial}{\partial t} + \vec{v}_{Ci}\cdot\nabla)\,\vec{v}_i = \frac{q_i}{m_i}(\vec{E} + \vec{v}_i \times \vec{B}) + \vec{g} - \frac{1}{m_i n_i}(\nabla p_i + \nabla\cdot\pi_i) \tag{6.34}$$

$$\frac{d_e}{dt}\vec{v}_e = (\frac{\partial}{\partial t} + \vec{v}_{Ce}\cdot\nabla)\,\vec{v}_e = \frac{q_e}{m_e}(\vec{E} + \vec{v}_e \times \vec{B}) + \vec{g} - \frac{1}{m_e n_e}(\nabla p_e + \nabla\cdot\pi_e) \tag{6.35}$$

$$(\frac{\partial}{\partial t} + \vec{v}_{Ci}\cdot\nabla)\, n_i + n_i \;\; \nabla\cdot\vec{v}_i = 0 \tag{6.36}$$

$$(\frac{\partial}{\partial t} + \vec{v}_{Ce}\cdot\nabla)\, n_e + n_e \;\; \nabla\cdot\vec{v}_e = 0 \tag{6.37}$$

We suppose a small plasma β so that spatial and time derivatives of $\vec{B}$ can be neglected, that is we take a homogeneous magnetic field and use the electrostatic approximation:

$$\vec{B} = \vec{B}_o = B\,\vec{e}_z \;, \qquad \vec{E} = -\nabla\Phi \tag{6.38}$$

The fictitious gravitational acceleration is $\vec{g} = -g\vec{e}_y$. All velocities are twodimensional so that the motion is always perpendicular to the magnetic field. Furthermore we will neglect temperature gradients so that pressure gradients are expressed by density gradients. The ion diamagnetic drift velocity is then

$$\vec{v}_{*i} = -\frac{1}{q_i \cdot n_i}\,\frac{\nabla p_i \times \vec{B}}{B^2} = -\frac{kT_i}{m_i}\,\frac{m_i}{q_i B}\quad \frac{\nabla n_i}{n_i} \times \vec{e}_z$$

$$\vec{v}_{*i} = -\frac{v_{Ti}^2}{\Omega_i}\nabla \ln\, n_i \times \vec{e}_z = -\rho_i^2\Omega_i \nabla \ln\, n_i \times \vec{e}_z \tag{6.39}$$

Obviously $\nabla\cdot\vec{v}_{*i} = 0$ is satisfied at any time. The electron formulas are similar. The total time derivatives d_i/dt and de/dt contain the convective derivatives $\vec{v}_{Ci}\cdot\nabla$ and $\vec{v}_{Ce}\cdot\nabla$ that are related to mass convection. Because of the supposed constant magnetic field and constant temperature the convective velocities $\vec{v}_{Ci}$ and $\vec{v}_{Ce}$ must coincide with the velocities of the respective gyrocenters. Hence $\vec{v}_{Ci}$ and $\vec{v}_{Ce}$ do not include the diamagnetic drifts $\vec{v}_{*i}$ and $\vec{v}_{*e}$, for these cannot cause any mass convection. They only describe the effect that in between two adjacent fluid layers with different density of gyrocenters more particles must have a microscopic velocity in one direction than in the opposite one, so that a fictitious difference velocity arises. The total velocity is then

$$\vec{v}_i = \vec{v}_{Ci} + \vec{v}_{*i} \, , \; \vec{v}_e = \vec{v}_{Ce} + \vec{v}_{*e} \tag{6.40}$$

If all velocities are of the same order the difference between $\vec{v}$ and $\vec{v}_C$ must be taken into account. For $T_e = T_i$ the diamagnetic drifts of electrons and ions are equal but opposite, $\vec{v}_{*e} = -\vec{v}_{*i}$. Nevertheless the mass convection can take place jointly provided that the gyrocenters move at almost equal speeds, $\vec{v}_{Ci} \approx \vec{v}_{Ce}$, and just this property is very typical and characteristic for convective cells in the plasma.

The ion gyroviscosity tensor π_i describes an averaging of the electrostatic force over the ion gyro orbit. The reduction effect is of the order of $k_\perp^2\rho_i^2 = k_\perp^2 v_{Ti}^2/\Omega_i^2$ and is supposed to be $<<1$. In cartesian coordinates the part of the gyroviscosity tensor perpendicular to the magnetic field has the following form:

$$\pi_{ixx} = - \pi_{iyy} = - \frac{p_i}{2\Omega_i} \left(\frac{\partial v_{ix}}{\partial y} + \frac{\partial v_{iy}}{\partial x}\right) \tag{6.41}$$

$$\pi_{ixy} = \pi_{iyx} = \frac{p_i}{2\,\Omega_i} \left(\frac{\partial v_{ix}}{\partial x} - \frac{\partial v_{iy}}{\partial y}\right) \tag{6.42}$$

$$\text{with} \quad \frac{p_i}{2\,\Omega_i} = \frac{v_{Ti}^2}{2\,\Omega_i} m_i n_i = \frac{1}{2} \rho_i^2 \Omega_i m_i n_i \tag{6.43}$$

In the equation of motion of the electrons (6.35) we can neglect all inertial and gyroterms and also $\vec{g}$ because of the smallness of the electron mass m_e. The remaining equation is

$$\vec{E} + \vec{v}_e \times \vec{B} - \frac{1}{q_e n_e} \nabla p_e = 0 \tag{6.44}$$

$$\vec{v}_e = \frac{\vec{E} \times \vec{B}}{B^2} - \frac{1}{q_e n_e} \frac{\nabla p_e \times \vec{B}}{B^2} = -\frac{1}{B} \nabla\Phi \times \vec{e}_z + \vec{v}_{*e} \tag{6.45}$$

$$\vec{v}_e = \vec{v}_E + \vec{v}_{*e} , \quad \vec{v}_E = -\frac{1}{B} \nabla\Phi \times \vec{e}_z \tag{6.46}$$

(6.40) and (6.46) show that for electrons the convective velocity $\vec{v}_{Ce}$ is identical to the electric drift velocity $\vec{v}_E$. Obviously $\nabla\cdot\vec{v}_E = 0$ is satisfied at any time. The continuity equation for the electrons (6.37) is therefore reduced to

$$(\frac{\partial}{\partial t} + \vec{v}_E \cdot \nabla)\, n_e = 0 \tag{6.47}$$

In equilibrium we suppose vanishing $\vec{E}$ and $\vec{v}_E$, so that $\vec{E}$ consists only of the perturbed field $\delta\vec{E}$ and consequently $\vec{v}_E$ is equal to the velocity variation $\delta\vec{v}_E$.

With regard to the ion motion, let us first consider the case of equilibrium. We take

$$\frac{\nabla n_i}{n_i} = \kappa \vec{e}_y = \text{const} \tag{6.48}$$

then
$$\vec{v}_i = \frac{m_i}{q_i} \frac{\vec{g} \times \vec{B}}{B^2} - \frac{1}{q_i n_i} \frac{\nabla p_i \times \vec{B}}{B^2} = \text{const}$$

$$= \frac{1}{\Omega_i} \vec{g} \times \vec{e}_z - \frac{v_{Ti}^2}{\Omega_i} \kappa \vec{e}_y \times \vec{e}_z$$

$$\vec{v}_i = -\frac{1}{\Omega_i} (g + v_{Ti}^2 \kappa)\, \vec{e}_x = \vec{v}_{Gi} + \vec{v}_{*i} \tag{6.49}$$

Inertial and gyroterms vanish. (6.40) and (6.49) show that in equilibrium the convective velocity $\vec{v}_{Ci}$ is identical to the gravitational drift velocity $\vec{v}_{Gi}$. Now we superpose a perturbation and substitute

$$\vec{v}_i \rightarrow \vec{v}_i + \delta\vec{v}_i = \vec{v}_{Gi} + \vec{v}_{*i} + \delta\vec{v}_{Ci} + \delta\vec{v}_{*i} \tag{6.50}$$

$$n_i \rightarrow n_i + \delta n_i , \quad n_e \rightarrow n_e + \delta n_e \tag{6.51}$$

At this point it is convenient to introduce a scaling or ordering system, that must be consistent with the properties of the Rayleigh-Taylor instabilities as discussed in chapter 6.1. At first we define $h = 2\,\Delta y$ as the width of the localization interval (which corresponds in the hydrodynamic model to the thickness of the boundary layer) and relate all other lengths to this length unit. The smallness parameter ε_* may then analogous to (5.46) be defined as

$$\frac{\kappa h}{\pi} = \varepsilon_* << 1 \tag{6.52}$$

This means that h must again be small against the scale length of the density gradient. That one in turn must be small against the curvature radius of the field lines:

$$\frac{1}{\kappa R} \sim \varepsilon_* , \quad \frac{h}{\pi R} \sim \varepsilon_*^2 \tag{6.53}$$

Spatial derivatives of the perturbed quantities and wavenumbers must be of the same order as π/h:

$$\frac{h}{\pi} \left(\frac{\partial}{\partial x} , \frac{\partial}{\partial y} , k_x, k_y\right) \sim 1 \tag{6.54}$$

In view of (6.17) the ion gyro radius, however, must be smaller than h:

$$r_i^2 k_\perp^2 \sim r_i^2 \frac{\pi^2}{h^2} \sim \varepsilon_* , \quad \frac{r_i}{h} \sim \frac{\sqrt{\varepsilon_*}}{\pi} \tag{6.55}$$

Time derivatives we will assume as being of second order compared with the ion gyro frequency:

$$\frac{\partial}{\Omega_i \partial t} \sim \varepsilon_*^2 \tag{6.56}$$

The ion drift velocity, too, results to be of second order:

$$v_{*i} = \Omega_i r_i^2 \kappa = \Omega_i \frac{r_i^2 \pi^2}{h^2} \frac{\kappa h}{\pi} \frac{h}{\pi} \sim \varepsilon_*^2 \frac{\Omega_i h}{\pi} \tag{6.57}$$

As a consequence of (6.52) we also must have

$$\frac{\delta n_i}{n_i} \sim \varepsilon_* \tag{6.58}$$

From (6.51) we then derive

$$\frac{\nabla n_i}{n_i} = \nabla \ln n_i \rightarrow \nabla \ln (n_i + \delta n_i)$$

$$= \nabla (\ln n_i + \frac{\delta n_i}{n_i} + \ldots)$$

$$= \kappa \vec{e}_y + \nabla \frac{\delta n_i}{n_i} + \ldots \sim \varepsilon_\star \frac{\pi}{h} \qquad (6.59)$$

The equilibrium density gradient as well as the associated perturbed quantity are of first order in $\varepsilon_\star$, the higher order terms of the series expansion don't come into play. We may then supplement (6.57) by

$$\delta \vec{v}_{\star i} \sim \varepsilon_\star^2 \frac{\Omega_i h}{\pi} \qquad (6.60)$$

According to (6.54) and (6.56) we consider convective velocities that are likewise of second order

$$\delta \vec{v}_{Ci} \sim \delta \vec{v}_E \sim \varepsilon_\star^2 \frac{\Omega_i h}{\pi} \qquad (6.61)$$

Only the gravitational drift, because of (6.53), results to be of third order:

$$v_{Gi} = \frac{g}{\Omega_i} \sim \frac{T_e}{T_i} \frac{v_{Ti}^2}{\Omega_i R} = \frac{T_e}{T_i} \frac{v_{\star i}}{\kappa R} \sim \varepsilon_\star^3 \frac{T_e}{T_i} \frac{\Omega_i h}{\pi} \qquad (6.62)$$

Our scaling is closely related to the well known FLR(Finite Larmor Radius) scaling, and it takes into account the special geometrical requirements of our localized convective cells. This careful $\varepsilon_\star$-ordering constitutes a major difference between our work and the treatment of the convective cells by Pavlenko and Weiland /16/. Another important difference consists in the fact that Pavlenko and Weiland consider the nonlinear excitation of convective cells on condition that the interchange modes are stable, whereas we consider the nonlinear saturation of convective cells on condition that the interchange modes are unstable.

It is convenient to write the gyroviscosity as $\pi = p \cdot \hat{\pi}$ and to define

$$\vec{Y} = \frac{1}{m_i n_i} \nabla \cdot \pi_i = \frac{kT_i}{m_i n_i} \nabla \cdot n_i \hat{\pi}_i = \frac{kT_i}{m_i} \left(\frac{\nabla n_i}{n_i} \cdot \hat{\pi}_i + \nabla \cdot \hat{\pi}_i\right)$$

$$\delta\vec{Y} = \frac{kT_i}{m_i}\left[\left(\frac{\nabla n_i}{n_i} + \nabla\frac{\delta n_i}{n_i}\right)\cdot\delta\hat{\pi}_i + \nabla\cdot\delta\hat{\pi}_i\right] \tag{6.63}$$

With this definition the perturbed form of the equation of motion (6.34) for the ions reads

$$\left[\frac{\partial}{\partial t} + (\vec{v}_{Gi} + \delta\vec{v}_{Ci})\cdot\nabla\right]\delta\vec{v}_i = \frac{q_i}{m_i}(\delta\vec{E} + \delta\vec{v}_i \times \vec{B}) - \frac{kT_i}{m_i}\nabla\frac{\delta n_i}{n_i} - \delta\vec{Y} \tag{6.64}$$

Up to second order in the ε_*-scaling this yields

$$\delta\vec{v}_i = \delta\vec{v}_E + \delta\vec{v}_{*i} = \frac{\delta\vec{E}\times\vec{B}}{B^2} - \frac{kT_i}{q_i B^2}\nabla\frac{\delta n_i}{n_i}\times\vec{B}$$

$$= -\left(\frac{1}{B}\nabla\delta\Phi + \frac{v_{Ti}^2}{\Omega_i}\nabla\frac{\delta n_i}{n_i}\right)\times\vec{e}_z = -\nabla\delta U \times \vec{e}_z \tag{6.65}$$

with the abbreviation

$$\delta U = \frac{\delta\Phi}{B} + \frac{v_{Ti}^2}{\Omega_i}\frac{\delta n_i}{n_i} \tag{6.66}$$

The velocity components are

$$\delta v_{ix} = -\frac{\partial}{\partial y}\delta U\ , \quad \delta v_{iy} = \frac{\partial}{\partial x}\delta U \tag{6.67}$$

so that (6.41) and (6.42) take the form

$$2\,\Omega_i\,\delta\hat{\pi}_{ixx} = -2\,\Omega_i\delta\hat{\pi}_{iyy} = -\left(\frac{\partial^2}{\partial x^2} - \frac{\partial^2}{\partial y^2}\right)\delta U \tag{6.68}$$

$$2\,\Omega_i\,\delta\hat{\pi}_{ixy} = 2\,\Omega_i\delta\hat{\pi}_{iyx} = -2\frac{\partial^2}{\partial x\partial y}\delta U \tag{6.69}$$

Now we can calculate the tensor divergence:

$$2\,\Omega_i\nabla\cdot\delta\hat{\pi}_i = 2\,\Omega_i\left(\frac{\partial}{\partial x}\delta\hat{\pi}_{ixx} + \frac{\partial}{\partial y}\delta\hat{\pi}_{ixy}, \frac{\partial}{\partial x}\delta\hat{\pi}_{ixy} + \frac{\partial}{\partial y}\delta\hat{\pi}_{iyy}\right)$$

$$= -\left(\frac{\partial}{\partial x}\left(\frac{\partial^2}{\partial x^2} - \frac{\partial^2}{\partial y^2}\right) + \frac{\partial}{\partial y}\left(2\frac{\partial^2}{\partial x\partial y}\right), \frac{\partial}{\partial x}\left(2\frac{\partial^2}{\partial x\partial y}\right) - \frac{\partial}{\partial y}\left(\frac{\partial^2}{\partial x^2} - \frac{\partial^2}{\partial y^2}\right)\right)\delta U$$

$$= -\left(\left(\frac{\partial^2}{\partial x^2} + \frac{\partial^2}{\partial y^2}\right)\frac{\partial}{\partial x}, \left(\frac{\partial^2}{\partial x^2} + \frac{\partial^2}{\partial y^2}\right)\frac{\partial}{\partial y}\right)\delta U = -\Delta(\nabla\delta U) \tag{6.70}$$

The lowest order gyroviscous correction is thus found to be

$$\delta\vec{Y} = \frac{kT_i}{m_i} \nabla \cdot \delta\hat{\pi}_i = -\frac{1}{2}\frac{kT_i}{m_i\Omega_i} \Delta(\nabla\delta U) \tag{6.71}$$

and from (6.64) follows up to third order

$$\delta\vec{v}_i = -\left(1 - \frac{1}{2}\frac{kT_i}{q_i B\Omega_i}\Delta\right) \nabla\delta U \times \vec{e}_z = -\left(1 - \frac{1}{2} r_i^2 \Delta\right) \nabla\delta U \times \vec{e}_z \tag{6.72}$$

Here we see clearly the effect of averaging the force over the gyro orbit. This effect is responsible for the gyro stabilization, not the diamagnetic Larmor drift as such. Since the force is expressed by a gradient, we can remove it by applying the curl-operator on the perturbed equation of motion (6.64). Let us first calculate $\nabla \times \delta\vec{Y}$, put $\delta\hat{n}_i = \delta n_i/n_i$, and consider the lowest order of

$$\nabla \times \left[2\,\Omega_i\, \nabla\delta\hat{n}_i \cdot \delta\hat{\pi}_i\right] =$$

$$= -\nabla \times \Big[\frac{\partial}{\partial x}\delta\hat{n}_i \cdot \left(\frac{\partial^2}{\partial x^2} - \frac{\partial^2}{\partial y^2}\right)\delta U + \frac{\partial}{\partial y}\delta\hat{n}_i \cdot \left(2\frac{\partial^2}{\partial x\partial y}\right)\delta U\,,$$

$$\frac{\partial}{\partial x}\delta\hat{n}_i \cdot \left(2\frac{\partial^2}{\partial x\partial y}\right)\delta U + \frac{\partial}{\partial y}\delta\hat{n}_i \cdot \left(\frac{\partial^2}{\partial x^2} - \frac{\partial^2}{\partial y^2}\right)\delta U\Big] \tag{6.73}$$

This rotation has only a z-component:

$$-\left(\frac{\partial}{\partial x}[\,]_y - \frac{\partial}{\partial y}[\,]_x\right) =$$

$$= \left(\frac{\partial^2}{\partial x^2} - \frac{\partial^2}{\partial y^2}\right)\delta U \cdot \left(2\frac{\partial^2}{\partial x\partial y}\right)\delta\hat{n}_i - \left(\frac{\partial^2}{\partial x^2} - \frac{\partial^2}{\partial y^2}\right)\delta\hat{n}_i \cdot \left(2\frac{\partial^2}{\partial x\partial y}\right)\delta U$$

$$-\frac{\partial}{\partial x}\delta\hat{n}_i \cdot \left(\frac{\partial^2}{\partial x^2} + \frac{\partial^2}{\partial y^2}\right)\frac{\partial}{\partial y}\delta U + \frac{\partial}{\partial y}\delta\hat{n}_i \left(\frac{\partial^2}{\partial x^2} + \frac{\partial^2}{\partial y^2}\right)\frac{\partial}{\partial x}\delta U$$

$$= 2\,\{\delta U, \delta\hat{n}_i\} + \nabla\delta\hat{n}_i \cdot \Delta\delta\vec{v}_i \tag{6.74}$$

where we have used (6.67) and defined the curly bracket as

$$\{\delta U, \delta\hat{n}_i\} = \left(\frac{\partial^2}{\partial x^2} - \frac{\partial^2}{\partial y^2}\right)\delta U \cdot \frac{\partial^2}{\partial x\partial y}\delta\hat{n}_i - \left(\frac{\partial^2}{\partial x^2} - \frac{\partial^2}{\partial y^2}\right)\delta\hat{n}_i \cdot \frac{\partial^2}{\partial x\partial y}\delta U \tag{6.75}$$

From (6.66) it follows

$$\{\delta U, \delta\hat{n}_i\} = \{\frac{\delta\Phi}{B}, \delta\hat{n}_i\} \tag{6.76}$$

Combining (6.63), (6.70) and (6.74) we get

$$\nabla \times \delta\vec{Y} = \frac{kT_i}{2m_i\Omega_i} \nabla \times 2\Omega_i \left[(\kappa\vec{e}_y + \nabla\delta\hat{n}_i) \cdot \delta\hat{\pi}_i\right]$$

$$= \frac{1}{2} r_i^2\Omega_i\vec{e}_c \left[2 \{\frac{\delta\Phi}{B}, \delta\hat{n}_i\} + (\kappa\vec{e}_y + \nabla\delta\hat{n}_i) \cdot \Delta\delta\vec{v}_i\right] \tag{6.77}$$

Here all terms are of fourth order in the ε_*-scaling, higher order terms have been omitted. Next let us consider the inertial and Lorentz terms in (6.64). $\vec{v}_{Gi}$ will be neglected because of (6.62). We identify $\delta\vec{v}_{Ci} = \delta\vec{v}_E$ and $\delta\vec{v}_i = \delta\vec{v}_E + \delta\vec{v}_{*i}$ (up to second order), and we define

$$\delta\vec{w}_i = \nabla \times \delta\vec{v}_i , \quad \vec{\Omega}_i = \frac{q_i}{m_i}\vec{B} = \Omega_i\vec{e}_z \tag{6.78}$$

Then $\nabla \times \left[\delta\vec{v}_{Ci} \cdot \nabla\delta\vec{v}_i - \frac{q_i}{m_i}\delta\vec{v}_i \times \vec{B}\right] =$

$$= \nabla \times \left[(\nabla\delta\vec{v}_i) \cdot \delta\vec{v}_{Ci} - \delta\vec{v}_{Ci} \times (\nabla \times \delta\vec{v}_i) - \delta\vec{v}_i \times \vec{\Omega}_i\right]$$

$$= \nabla \times \left[(\nabla\delta\vec{v}_{*i}) \cdot \delta\vec{v}_E + \frac{1}{2}\nabla\delta\vec{v}_E^{\,2} - \delta\vec{v}_{Ci} \times \delta\vec{w}_i - \delta\vec{v}_i \times \vec{\Omega}_i\right]$$

$$= \nabla \times \delta\vec{Z} - \nabla \times \left[\delta\vec{v}_{Ci} \times \delta\vec{w}_i + \delta\vec{v}_i \times \vec{\Omega}_i\right]$$

$$= \nabla \times \delta\vec{Z} + (\nabla\cdot\delta\vec{v}_{Ci} + \delta\vec{v}_{Ci}\cdot\nabla)\,\delta\vec{w}_i + \nabla\cdot\delta\vec{v}_i\vec{\Omega}_i \tag{6.79}$$

Here we have used $\nabla\cdot\delta\vec{w}_i = \nabla\cdot\vec{\Omega}_i = 0$ and $\delta\vec{w}_i \| \vec{\Omega}_i \| \vec{e}_z$ and the vanishing of gradients in the z-direction. Taking into account terms up to fourth order in (6.79) we may neglect $\nabla\cdot\delta\vec{v}_{Ci}\cdot\delta\vec{w}_i$, but we must include $\nabla\cdot\delta\vec{v}_i\vec{\Omega}_i$. First we evaluate $\nabla\times\delta\vec{Z}$:

$$\nabla \times \delta\vec{Z} = \nabla \times \left[(\nabla\delta\vec{v}_{*i}) \cdot \delta\vec{v}_E\right] =$$

$$= r_i^2\Omega_i \nabla \times \left[\nabla (\nabla \frac{\delta\Phi}{B} \cdot \nabla\delta\hat{n}_i)\right]$$

$$= r_i^2\Omega_i \nabla \times \left[-\frac{\partial}{\partial x}\frac{\delta\Phi}{B}\frac{\partial^2}{\partial x^2}\delta\hat{n}_i + \frac{\partial}{\partial y}\frac{\delta\Phi}{B}\frac{\partial^2}{\partial x\partial y}\delta\hat{n}_i ,\right.$$

$$\frac{\partial}{\partial x}\frac{\delta\Phi}{B}\frac{\partial^2}{\partial x\partial y}\delta\hat{n}_i + \frac{\partial}{\partial y}\frac{\delta\Phi}{B}\frac{\partial^2}{\partial y^2}\delta\hat{n}_i \Big]$$

$$= r_i^2\vec{\Omega}_i \left(\frac{\partial}{\partial x}[\,]_y - \frac{\partial}{\partial y}[\,]_x\right) = r_i^2\vec{\Omega}_i \{\frac{\delta\Phi}{B}, \delta\hat{n}_i\} \qquad (6.80)$$

Now combining (6.64), (6.77), (6.79) and (6.80) we find as an intermediate result

$$\left(\frac{\partial}{\partial t} + \delta\vec{v}_E\cdot\nabla\right)\delta\vec{w}_i + \nabla\cdot\delta\vec{v}_i\vec{\Omega}_i = -\, r_i^2\vec{\Omega}_i\Big[2\,\{\frac{\delta\Phi}{B}, \delta\hat{n}_i\}$$

$$+ \frac{1}{2}(\kappa\vec{e}_y + \nabla\delta\hat{n}_i)\cdot\Delta\delta\vec{v}_i\Big] \qquad (6.81)$$

For the calculation of $\nabla\cdot\delta\vec{v}_i$ we need the perturbed forms of the continuity equations for the ions (6.36) and the electrons (6.47):

$$\left[\frac{\partial}{\partial t} + (\vec{v}_{Gi} + \delta\vec{v}_{Ci})\cdot\nabla\right]\ln(n_i+\delta n_i) + \nabla\cdot\delta\vec{v}_i = 0 \qquad (6.82)$$

$$\left[\frac{\partial}{\partial t} + \delta\vec{v}_E\cdot\nabla\right]\ln(n_e+\delta n_e) = 0 \qquad (6.83)$$

By virtue of the quasineutrality condition we may set $n_i = n_e = n$ and also $\delta n_i = \delta n_e = \delta n$. Subtracting (6.83) from (6.82) yields

$$(\vec{v}_{Gi}+\delta\vec{v}_{Ci}-\delta\vec{v}_E)\cdot\nabla\ln(n+\delta n) + \nabla\cdot\delta\vec{v}_i = 0 \qquad (6.84)$$

This requires the expansion of $\delta\vec{v}_{Ci}$ up to third order. Using (6.72) and (6.65) we find

$$\begin{aligned}\delta\vec{v}_{Ci}-\delta\vec{v}_E &= \delta\vec{v}_i-\delta\vec{v}_E-\delta\vec{v}_{*i}\\ &= \left(1-\frac{1}{2}r_i^2\,\Delta\right)(\delta\vec{v}_E+\delta\vec{v}_{*i}) - \delta\vec{v}_E-\delta\vec{v}_{*i}\\ &= -\frac{1}{2}r_i^2\,\Delta\,(\delta\vec{v}_E+\delta\vec{v}_{*i}) = -\frac{1}{2}r_i^2\,\Delta\delta\vec{v}_i\end{aligned} \qquad (6.85)$$

so that (6.84) takes the form

$$\begin{aligned}\nabla\cdot\delta\vec{v}_i &= \left(-\vec{v}_{Gi} + \frac{1}{2}r_i^2\,\Delta\delta\vec{v}_i\right)\cdot(\kappa\vec{e}_y + \nabla\delta\hat{n})\\ &= -\vec{v}_{Gi}\cdot\nabla\delta\hat{n} + \frac{1}{2}r_i^2\Delta\delta\vec{v}_i\cdot(\kappa\vec{e}_y+\nabla\delta\hat{n})\end{aligned} \qquad (6.86)$$

We see that the divergence of the ion velocity is small of fourth order but finite. This remains true even for vanishing r_i. The compressibility of the ions in our two-fluid model is essential for the formation and growth of vortices by the action of gravity, as is evident from equations (6.81) and (6.86). Remember that $\delta\vec{w}_i = \nabla x \delta\vec{v}_i$ describes the vorticity. In a one-fluid model, as was treated in our liquid boundary layer and quite similarly in an ideal MHD-description of the plasma, one usually assumes strict incompressibilitiy of the fluid. This means that there must be another source of vorticity. It can be shown that the essential agent in such cases is a finite baroclinic vector $\nabla p x \nabla n = nk \nabla T x \nabla n$, whereas we have assumed an isothermal plasma. Hence the physics of the two-fluid model is basically different from the one-fluid model. As a consequence the two-fluid model may allow weak instability even in cases where pure MHD would predict complete stability. It is this weak instability that causes the convective diffusion.

Next we substitute (6.86) into (6.81), use

$$\delta\vec{w}_i = \nabla \times (-\nabla\delta U \times \vec{e}_z) = \Delta\delta U \, \vec{e}_z \tag{6.87}$$

and take the scalar product with $\vec{e}_z$:

$$\left(\frac{\partial}{\partial t} + \delta\vec{v}_E\cdot\nabla\right) \Delta \left(\frac{\delta\Phi}{B} + r_i^2\Omega_i\delta\hat{n}\right) - \vec{v}_{Gi}\cdot\nabla\delta\hat{n}\Omega_i =$$

$$= -r_i^2\Omega_i\left[2\left\{\frac{\delta\Phi}{B}, \delta\hat{n}\right\} + (\kappa\vec{e}_y+\nabla\delta\hat{n}) \cdot \Delta\delta\vec{v}_i\right] \tag{6.88}$$

This is further simplified by applying the Laplace operator on the electron continuity equation (6.83):

$$\left(\frac{\partial}{\partial t} + \delta\vec{v}_E \cdot \nabla\right) \delta\hat{n} + \delta\vec{v}_E \cdot \kappa\vec{e}_y = 0 \tag{6,89}$$

$$\left(\frac{\partial}{\partial t} + \delta\vec{v}_E \cdot \nabla\right) \Delta\delta\hat{n} + \Delta\delta\vec{v}_E \cdot (\nabla\delta\hat{n}+\kappa\vec{e}_y) =$$

$$= -2 \left(\nabla\delta v_{Ex} \cdot \nabla \frac{\partial}{\partial x} \delta\hat{n} + \nabla\delta v_{Ey} \cdot \nabla \frac{\partial}{\partial y} \delta\hat{n}\right)$$

$$= -2 \left(- \frac{\partial^2}{\partial x\partial y} \frac{\delta\Phi}{B} \frac{\partial^2}{\partial x^2} \delta\hat{n} - \frac{\partial^2}{\partial y^2} \frac{\delta\Phi}{B} \frac{\partial^2}{\partial x\partial y} \delta\hat{n}\right.$$

$$+ \frac{\partial^2}{\partial x^2} \frac{\delta\Phi}{B} \frac{\partial^2}{\partial x \partial y} \delta\hat{n} + \frac{\partial^2}{\partial x \partial y} \frac{\delta\Phi}{B} \frac{\partial^2}{\partial y^2} \delta\hat{n})$$

$$= -2 \left\{\frac{\delta\Phi}{B}, \delta\hat{n}\right\} \tag{6.90}$$

Multiplying (6.90) by $r_i^2 \Omega_i$ and subtracting from (6.88) yields finally the result

$$(\frac{\partial}{\partial t} + \delta\vec{v}_E \cdot \nabla) \Delta \frac{\delta\Phi}{B} - \Omega_i \vec{v}_{Gi} \cdot \nabla\delta\hat{n} + r_i^2 \Omega_i (\kappa\vec{e}_y + \nabla\delta\hat{n}) \cdot \Delta\delta\vec{v}_{*i} = 0 \tag{6.91}$$

Apart from the FLR-scaling no additional assumptions have been made, so that (6.91) is correct up to higher order terms in ε_*. Equations (6.89) and (6.91) constitute a system of nonlinear differential equations for the evolution of the electrostatic potential $\delta\Phi$ and the relative density variation $\delta\hat{n} = \delta n/n$. Let us now restrict the generality by introducing an assumption that has been made plausible in the discussion of chapter 6.1. We assume that one ground made is distinguished among all other modes by its higher growth rate, so that competing harmonics remain smaller say by one order in ε_*. Then we may put $\Delta\delta\hat{n} = - k_\perp^2 \delta\hat{n}$ and get

$$\begin{aligned}
\Delta\delta\vec{v}_{*i} \cdot (\kappa\vec{e}_y + \nabla\delta\hat{n}) &= \Delta(-r_i^2 \Omega_i \nabla\delta\hat{n} \times \vec{e}_z) \cdot (\kappa\vec{e}_y + \nabla\delta\hat{n}) \\
&= + k_\perp^2 r_i^2 \Omega_i \nabla\delta\hat{n} \times \vec{e}_z \cdot (\kappa\vec{e}_y + \nabla\delta\hat{n}) \\
&= - k_\perp^2 r_i^2 \Omega_i \kappa\vec{e}_y \times \vec{e}_z \cdot \nabla\delta\hat{n} = k_\perp^2 \vec{v}_{*i} \cdot \nabla\delta\hat{n}
\end{aligned} \tag{6.92}$$

The equations (6.91) and (6.89) are thus reduced to

$$(\frac{\partial}{\partial t} + \partial\vec{v}_E \cdot \nabla) \Delta \frac{\delta\Phi}{B} + (g - k_\perp^2 r_i^2 \Omega_i v_{*i}) \frac{\partial\delta\hat{n}}{\partial x} = 0 \tag{6.93}$$

$$(\frac{\partial}{\partial t} + \delta\vec{v}_E \cdot \nabla) \delta\hat{n} + \kappa \frac{\partial}{\partial x} \frac{\delta\Phi}{B} = 0 \tag{6.94}$$

There is a very remarkable similarity to the system of equations (5.17) and (5.18) of the hydrodynamic model, which will be exploited in the following.

6.3 Estimation of Maximum Anomalous Transport by Convective Diffusion

Let us first consider the linear approximation and drop the convective derivative $\delta\vec{v}_E \cdot \nabla$. Then we find from (6.93) and (6.94)

$$\frac{\partial^2}{\partial t^2} \Delta \frac{\delta\Phi}{B} + (g - k_\perp^2 r_i^2 \Omega_i v_{*i}) \frac{\partial}{\partial x} (-\kappa \frac{\partial}{\partial x} \frac{\delta\Phi}{B}) = 0 \qquad (6.95)$$

Since we have directed our attention to the ground mode, this reduces to

$$\left[-\frac{\partial^2}{\partial t^2} - \left(\frac{k_x^2 g\kappa}{k_\perp^2} - k_x^2 v_{*i}^2 \right) \right] \frac{\delta\Phi}{B} = 0 \qquad (6.96)$$

The solution grows as $e^{\sigma t}$ with

$$\sigma = \sqrt{\frac{k_x^2 \, g \, \kappa}{k_\perp^2} - k_x^2 v_{*i}^2} = \sqrt{\sigma_o^2 - \omega_{*i}^2} \qquad (6.97)$$

where $\sigma_o = \sqrt{k_x^2 g\kappa / k_\perp^2}$ is the growth rate in the absence of gyrostabilization and $\omega_{*i} = k_x v_{*i}$ is the ion drift frequency. We have thus found a purely exponential growth, with a growth rate that is reduced by the ion gyromotion. A real part of the frequency does not occur in the unstable case. In the marginal case the time dependence vanishes completely. This reflects the fact that convective cells are "zero frequency" modes, in contrast to drift modes, which possess always a real part of the frequency of the order of ω_{*e}. Electrons and ions move in convective cells jointly (up to order ε_*^2) with the electric drift velocity $\delta\vec{v}_E$, in complete analogy to the hydrodynamic model with twodimensional incompressible fluid motion. The equal and opposite (for $T_e = T_i$) Larmor drift of ions and electrons does not appear because it does not involve a real mass convection. We may compare (6.97) with the analogous expression (3.50) for the liquid boundary layer in the region of weak instability where the dynamic stabilization reduces the growth rate:

$$\mu = \sqrt{-a - \frac{1}{2} q^2} = \sqrt{\frac{4}{\omega^2} \frac{g}{l} - \frac{1}{2} \frac{4}{\omega^4} \frac{b_o^2}{l^2}}$$

or $$\sigma = \frac{\mu\omega}{2} = \sqrt{\frac{g}{l} - \frac{1}{2} \frac{b_o^2}{\omega^2 l^2}} \qquad (6.98)$$

The analogy is obvious if we write (6.97) in the form

$$\sigma = \frac{k_x}{k_\perp}\sqrt{g\kappa - k_\perp^2 r_i^2 \frac{(v_{Ti}^2/r_i)^2\ \kappa^2}{\Omega_i^2}} \tag{6.99}$$

In the plasma the fictitious gravitational acceleration is smaller than the acceleration by terrestrial gravity, and the stabilizing term is also smaller by the factor $k_\perp^2 r_i^2$ describing the averaging over the gyro orbit, but this does not impair the structural agreement of (6.98) and (6.99). Compared with the dispersion relation (6.9, 6.18, 6.19) discussed in chapter 6.1 we have removed the real part that pretends a propagation in drift direction with $\frac{1}{2}\ v_{*i}$. This also implies that under the root $\frac{1}{4}\ v_{*i}^2$ must be replaced by v_{*i}^2. Our new formulation should be more realistic in so far as it describes linked convective cells fixed in space just as in the liquid boundary layer. In the plasma we have the advantage that recourse to Mathieu functions is not necessary. Moreover, factors like $e^{-1/2\ \kappa y}$ (formerly $e^{-1/2\ \beta z}$) can be neglected from the beginning and approximated by unity, because they generate terms of higher order in ε_* which are omitted in the FLR-scaling. In the following, we write simply $\delta\vec{v}$ instead of $\delta\vec{v}_E$ and consider expansions of the form

$$\left.\begin{matrix}\delta v_y \\ \\ \delta\hat{n}\end{matrix}\right\} = \sum_{k_x,k_y}\left\{\begin{matrix}\delta V_{\vec{k}}(t) \\ \\ \delta N_{\vec{k}}(t)\end{matrix}\right\} \cos k_x x \cos k_y y \tag{6.100}$$

where we are interested only in the nonlinear selfinteraction of the ground mode. We assume free boundary surfaces at the edges of the localization interval and periodic boundary conditions in the x-direction, so that the configuration consists of two pairs of counterspinning eddies continuated and repeated many times in the drift direction. For the ground mode we have

$$\Delta \frac{\delta\Phi}{B} = \frac{\partial}{\partial x}\ \delta v_y - \frac{\partial}{\partial y}\ \delta v_x = \frac{k_\perp^2}{k_x^2}\frac{\partial}{\partial x}\ \delta v_y \tag{6.101}$$

and our basic equations (6.93, 6.94) are reduced to

$$\left(\frac{\partial}{\partial t} + \delta\vec{v}\cdot\nabla\right)\ \delta v_y = -\frac{k_x^2 g_*}{k_\perp^2}\ \delta\hat{n} \tag{6.102}$$

$$(\frac{\partial}{\partial t} + \delta\vec{v}\cdot\nabla)\ \delta\hat{n} = -\ \kappa\delta v_y \tag{6.103}$$

$$\text{with}\quad g_* = g - k_\perp^2 r_i^2 \Omega_i v_{*i} \tag{6.104}$$

This system is almost identical to the hydrodynamic equations (5.27, 5.28). One difference is the constant g_* in constrast to the time dependent $\gamma(t)$. We may increase the formal analogy of the plasma and the liquid systems by relating the FLR-ordering parameter ε_* to the former smallness parameter ε through the definitions

$$\beta = \varepsilon_* \kappa, \qquad \varepsilon = \frac{\beta h}{\pi} = \varepsilon_* \frac{\kappa h}{\pi} = \varepsilon_*^2$$

$$\gamma = \frac{g_*}{\varepsilon_*}, \qquad \delta\hat{\rho} = \varepsilon_* \delta\hat{n}, \qquad \delta S_{\vec{k}} = \varepsilon_* \delta N_{\vec{k}} \tag{6.105}$$

Instead of the former $1/\beta l$ we now use $k_x^2/k_\perp^2$, and the shake frequency is replaced by the gyrofrequency Ω_i. We are then in a position to repeat the calculations and results of chapter 5.2 for the ground mode and obtain the equivalent of (5.50) in the form

$$\delta\ddot{S}_{\vec{k}} + a\delta S_{\vec{k}} + \frac{1}{2}\psi^2 \delta S_{\vec{k}}^3 = 0 \tag{6.106}$$

$$\text{with}\quad a = -\frac{4}{\Omega_i^2}\,\frac{k_x^2\, g_* \kappa}{k_\perp^2} = -\frac{4\,\sigma^2}{\Omega_i^2} \tag{6.107}$$

$$\psi = -\frac{1}{\varepsilon}\,\frac{\frac{d}{d\tau}\, e^{\mu\tau}}{e^{\mu\tau}} = -\frac{\mu}{\varepsilon} = -\frac{\sqrt{-a}}{\varepsilon} \tag{6.108}$$

Note that the Mathieu function is now reduced to the simple exponential function $e^{\mu\tau}$. A stationary solution of (6.106) is obviously

$$\frac{1}{2}\psi^2 \delta S_{\vec{k}}^2 = -a, \qquad \delta S_{\vec{k}}^2 = \frac{-2a}{-a}\,\varepsilon^2$$

$$\delta S_{\vec{k}} = \pm\sqrt{2}\,\varepsilon\ , \qquad \delta N_{\vec{k}} = \pm\sqrt{2}\,\varepsilon_* \tag{6.109}$$

This determines the value of the saturation amplitude. It corresponds exactly to the two minima of the parabolic potential well of fourth order in fig. 8. This is not surprising, for g_* does not contain an oscillating part so that the coefficients of (6.106) are constant just as the coefficients of the differential equation (5.57).

Let us now estimate the maximum diffusion coefficient related to convective mass transport. We follow the calculation of chapter 5.4, use the representation (6.100) with

$$\delta V_{\vec{k}} = \Psi \delta S_{\vec{k}} = \frac{h}{T} \psi \delta S_{\vec{k}} = \frac{\Omega_i h}{2\pi} \psi \varepsilon_{\star} \delta N_{\vec{k}} \tag{6.110}$$

and $k_x = \frac{\pi}{D}$, $\quad k_y = \frac{\pi}{h}$ (6.111)

and apply (5.70) for the convective mass current density:

$$j_{con} = \frac{1}{D} \int_0^D m_i \delta n \delta v_y \, dx \tag{6.112}$$

$$= \frac{1}{D} m_i n_o \int_0^D \delta\hat{n} \delta v_y dx$$

$$= \frac{1}{2} m_i n_O \, \delta N_{\vec{k}} \delta V_{\vec{k}} \cos^2 k_y y$$

$$= \frac{1}{2} \varepsilon_{\star} m_i n_o \frac{\Omega_i h}{2\pi} \psi \delta N_{\vec{k}}^2 \cos^2 k_y y$$

$$j_{con} = - \frac{1}{2} \varepsilon_{\star} m_i n_o \frac{\Omega_i h}{2\pi} \frac{\mu}{\varepsilon} 2 \varepsilon \cos^2 k_y y$$

$$j_{con} = - \frac{\kappa h}{\pi} m_i n_o \frac{\Omega_i h \mu}{2 \pi} \cos^2 k_y y$$

$$= - m_i n_o' \frac{\Omega_i \mu}{2} \frac{h^2}{\pi^2} \cos^2 k_y y$$

$$j_{con} = - \mathcal{D} m_i n_o' \cos^2 k_y y \tag{6.113}$$

with $\mathcal{D} = \frac{\Omega_i \mu}{2} \frac{h^2}{\pi^2} = \sigma \frac{h^2}{\pi^2} = \frac{\sigma}{k_y^2}$ (6.114)

We recall that short wave instabilities such as drift instabilities can take the role of the parametric resonances and provide a complementary diffusion $\sim \sin^2 k_y y$. It is interesting to note that already Pfirsch /17/, by introducing the notion of turbulent eddies and localized vortices and the concept of Prandtl's mixing length theory into strong plasma turbulence, conjectured a diffusion coefficient of the order σl^2 in formal agreement with (6.114), the mixing length l (times π) being the equivalent of our localization width h.

To get an idea of the magnitude of the diffusion coefficient $\mathcal{D}$, we assume that $\sigma(\kappa)$ takes its maximum with respect to κ. Since the radicand in (6.99) has the form $g\kappa - f\kappa^2$, the maximum is reached for $g\kappa = 2\, f\kappa^2$. This maximum corresponds exactly to the "working point" $q = q_o/2$ on the straight line in fig. 4 for the hydrodynamic model. Referring to (6.97) we assume that $\sigma_o^2 = 2\,\omega_{*i}^2$, so that $\sigma = \omega_{*i}$. The maximum possible diffusion coefficient $\mathcal{D}$, that defines an upper bound for the anomalous diffusion induced by convection, is thus found to be

$$\mathcal{D} = \omega_{*i} \frac{h^2}{\pi^2} = k_x v_{*i} \frac{h^2}{\pi^2} = k_x \frac{kT_i}{q_i B} \frac{\kappa h^2}{\pi^2}$$

$$\mathcal{D} = \frac{\kappa h}{\pi} \frac{k_x}{k_y} \frac{kT_i}{q_i B} = \varepsilon_* \frac{k_x}{k_y} \frac{kT_i}{q_i B} \tag{6.115}$$

This may be compared with the Bohm diffusion coefficient

$$\mathcal{D}_{\mathrm{Bohm}} = \frac{1}{16} \frac{kT_i}{q_i B} \tag{6.116}$$

According to our discussion in chapter 6.1 we have $k_x \sim k_y$, while $\varepsilon_* = \kappa h/\pi = n_o'/n_o\, h/\pi$ is given by the ratio of the localization width to the scale length of the density gradient. Keeping in mind that the convective diffusion deforms a steady density profile into a sequence of stairs, so that κ is the stationary steepened κ in one single step, not the average $\bar{\kappa}$ of the initial density profile, we may estimate ε_* to be of the order of one over the total number of density steps, say 10^{-2}.

Since the n_o' occurring explicitly in j_{con} (6.113) is also the steepened gradient and not the average $\overline{n_o'}$, we conclude that the effective diffusion coefficient $\bar{\mathcal{D}} = n_o' \mathcal{D} / \overline{n_o'}$ is clearly greater than $\mathcal{D}$. Thus our maximal diffusion may well be of the order of Bohm diffusion.

REFERENCES

/1/ *Lord J.W. Rayleigh, "... Equilibrium of an Incompressible Heavy Fluid of Variable Density", Proc. London Math. Soc. XIV, p. 170 (1883)*

/2/ *G.H. Wolf, "Dynamic Stabilization of Hydrodynamic Interchange Instabilities - a Model for Plasma Physics", AIP Conference Proceedings No. 1, p. 293, New York (1970)*

/3/ *W. Hopmann, H. Gerhauser, G.H. Wolf, unpublished (1981)*

/4/ *J. Wesson, "Dynamic Stabilization and the Rayleigh-Taylor Instability", Phys. Fluids 13, p. 761 (1970)*

/5/ *J. Meixner, F.W. Schäfke, "Mathieusche Funktionen und Sphäroidfunktionen", Springer Berlin-Göttingen-Heidelberg (1954)*

/6/ *N.W. McLachlan, "Theory and Application of Mathieu Functions", Clarendon Press Oxford (1947)*

/7/ *H. Gerhauser, "Theoretische Analyse des turbulenten Transports durch die diffuse Grenzschicht bei der dynamischen Stabilisierung überschichteter mischbarer Flüssigkeiten", KFA-Report Jül-1645 (1980)*

/8/ *A.B. Mikhailovskii, "Oscillations of an Inhomogeneous Plasma", Reviews of Plasma Physics Vol. 3, p. 159, Consultants Bureau New York (1967)*

/9/ *A.B. Mikhailovskii, "Instabilities of an Inhomogeneous Plasma", Theory of Plasma Instabilities Vol. 2, Consultants Bureau New York-London (1974)*

/10/ *P.L. Similon, "A Renormalized Theory of Drift Wave Turbulence in Sheared Magnetic Fields", Dissertation Princeton University (August 1981)*

/11/ *B.B. Kadomtsev, A.V. Timofeev, "Drift Fluctuations in Nonhomogeneous Plasma in a Magnetic Field", Soviet Physics Doklady Vol. 7, p. 826 (1963)*

/12/ *A. Hasegawa, K. Mima, "Pseudo-three-dimensional Turbulence in Magnetized Nonuniform Plasma", Phys. Fluids 21, p. 87 (1978)*

/13/ *A. Rogister, G. Hasselberg, "Drift-Wave Spectra Obtained from the Theory of Nonlinear Ion-Landau Damping in Sheared Magnetic Fields", Phys. Rev. Letters 48, p. 249 (1982)*

/14/ *K. Mima, Y.C. Lee, "Modulational Instability of Strongly Dispersive Drift Waves and Formation of Convective Cells", Phys. Fluids 23, p. 105 (1980)*

/15/ *H.U. Rahman, "Generation of Vortex and Magnetostatic Turbulence in Plasmas", Sonderforschungsbereich Plasmaphysik Bochum/Jülich, Report 81-L1-88, Dissertation (Dec. 1981)*

/16/ *V.P. Pavlenko, J. Weiland, "Nonlinear Excitation of Convective Cells by Interchange Modes and Spectrum Cascade Processes", Phys. Fluids 23, p. 719 (1980)*

/17/ *D. Pfirsch, "Strong Turbulence in Collisionless Plasmas", Nonlinear Effects in Plasmas (Editors G. Kalman and M. Feix), p. 309, Gordon and Breach, New York - London - Paris (1969)*

/18/ *G.H. Wolf, Z. Physik 227, p. 291 (1969) and Phys. Rev. Letters 24, p. 444 (1970)*

Acknowledgements

A stimulating discussion with Dr. M. Lücke, several valuable discussions with Dr. H. Kever, and the constant interest and support by Prof. G.H. Wolf are gratefully acknowledged.

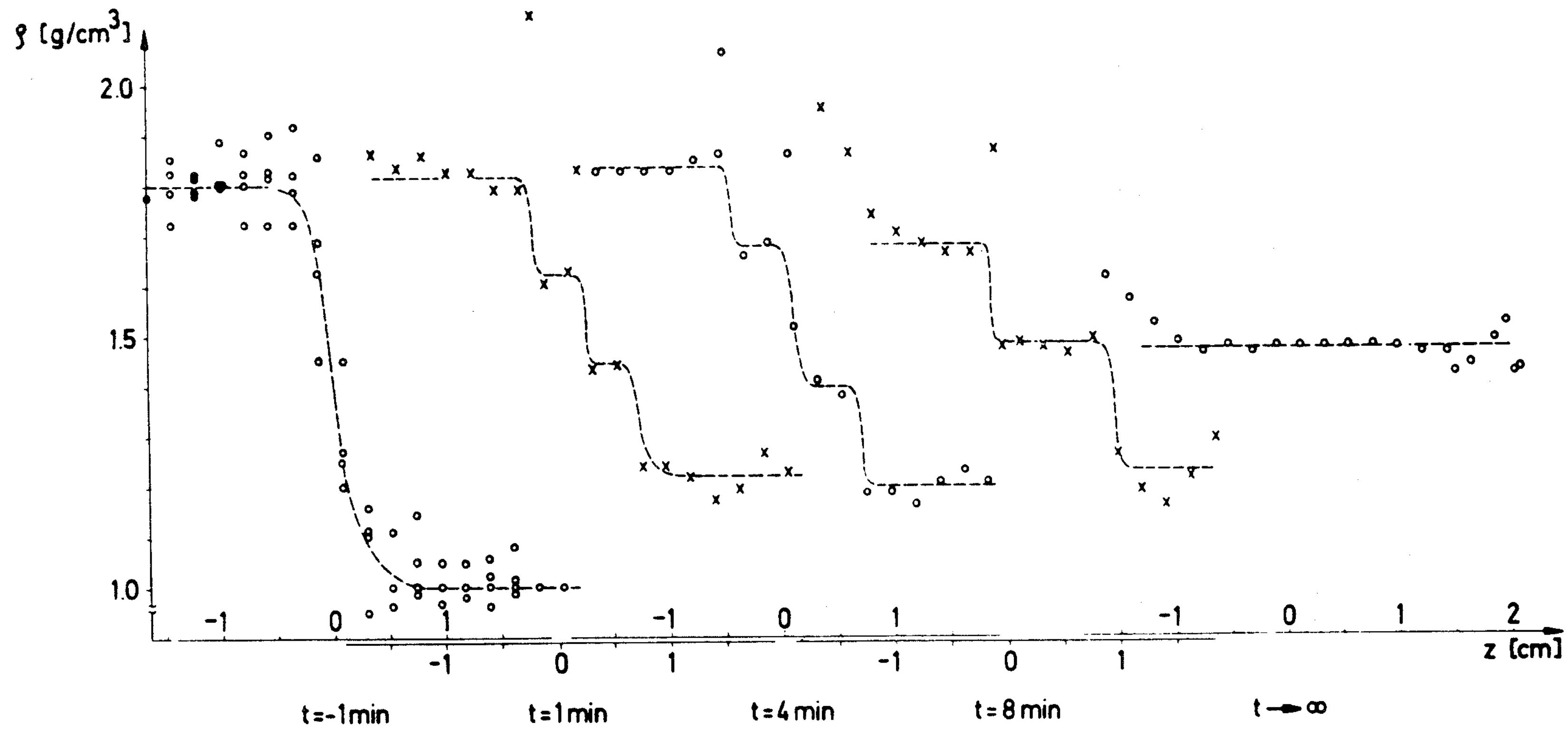

<u>Fig.1:</u> Evolution of density profiles between an aqueous ZnJ_2-solution (ϱ_2 = 1.8 g/cm^3, upper layer) and water (ϱ_1 = 1.0 g/cm^3), according to Wolf /2/.
D = 0.78 cm, Λ = 6 cm, b_o/g = 60, $\omega/2\pi$ = 100 Hz

Fig.2: Velocity field for (m,n) = (3,2)

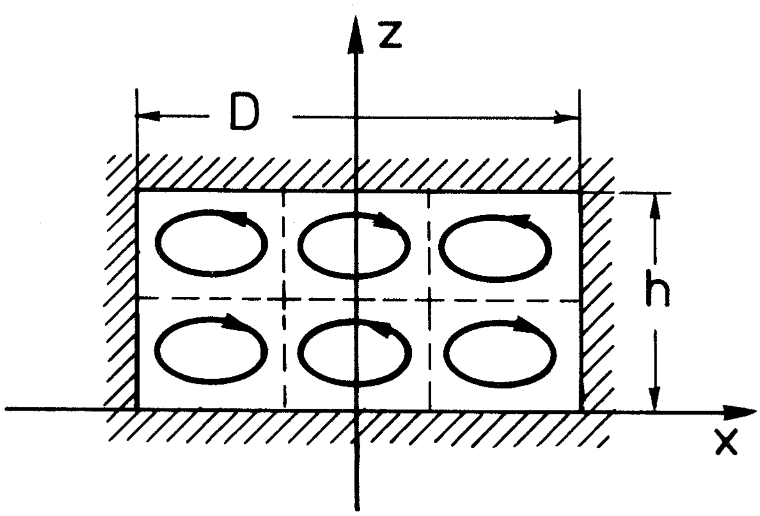

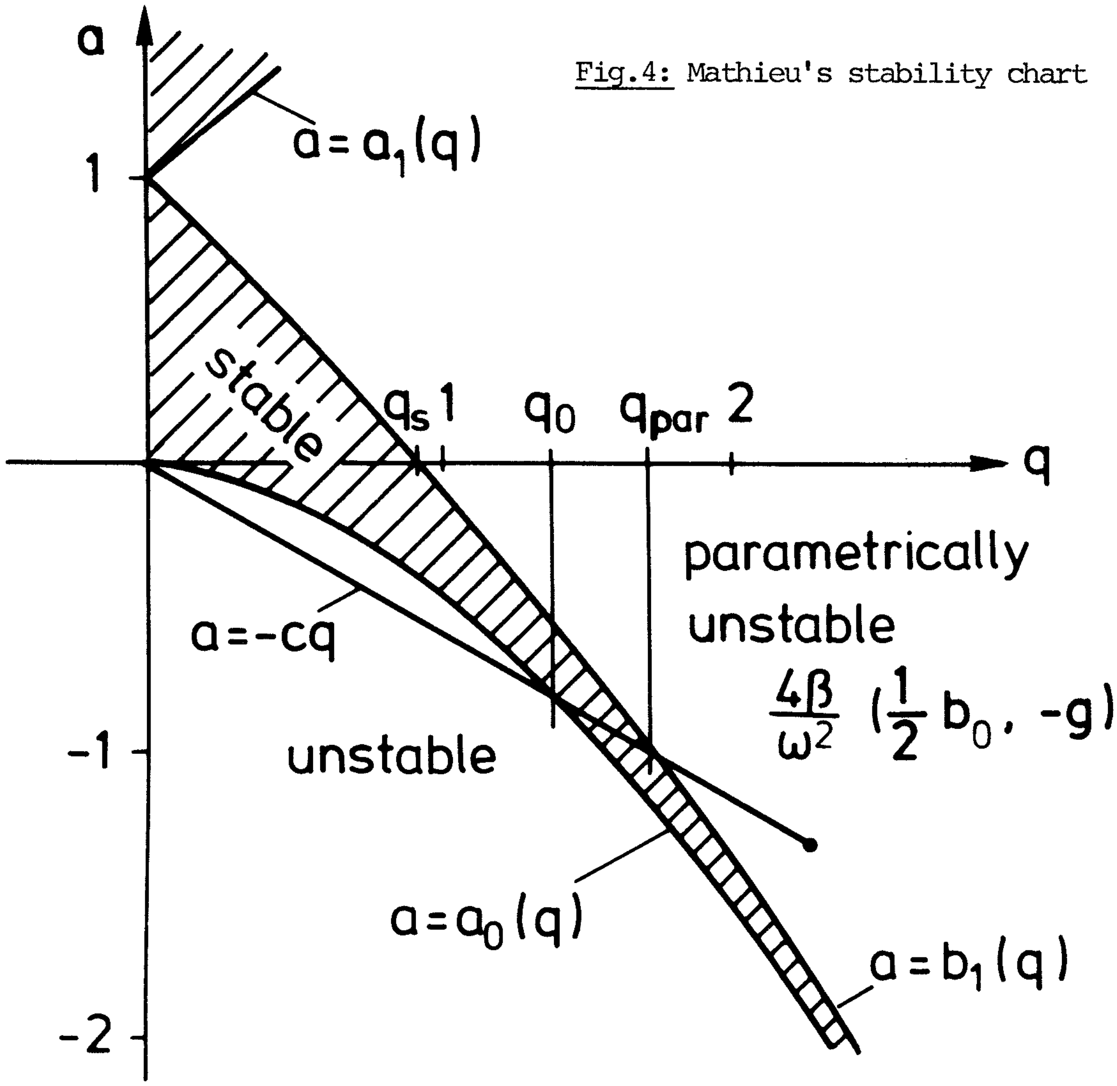

Fig.4: Mathieu's stability chart

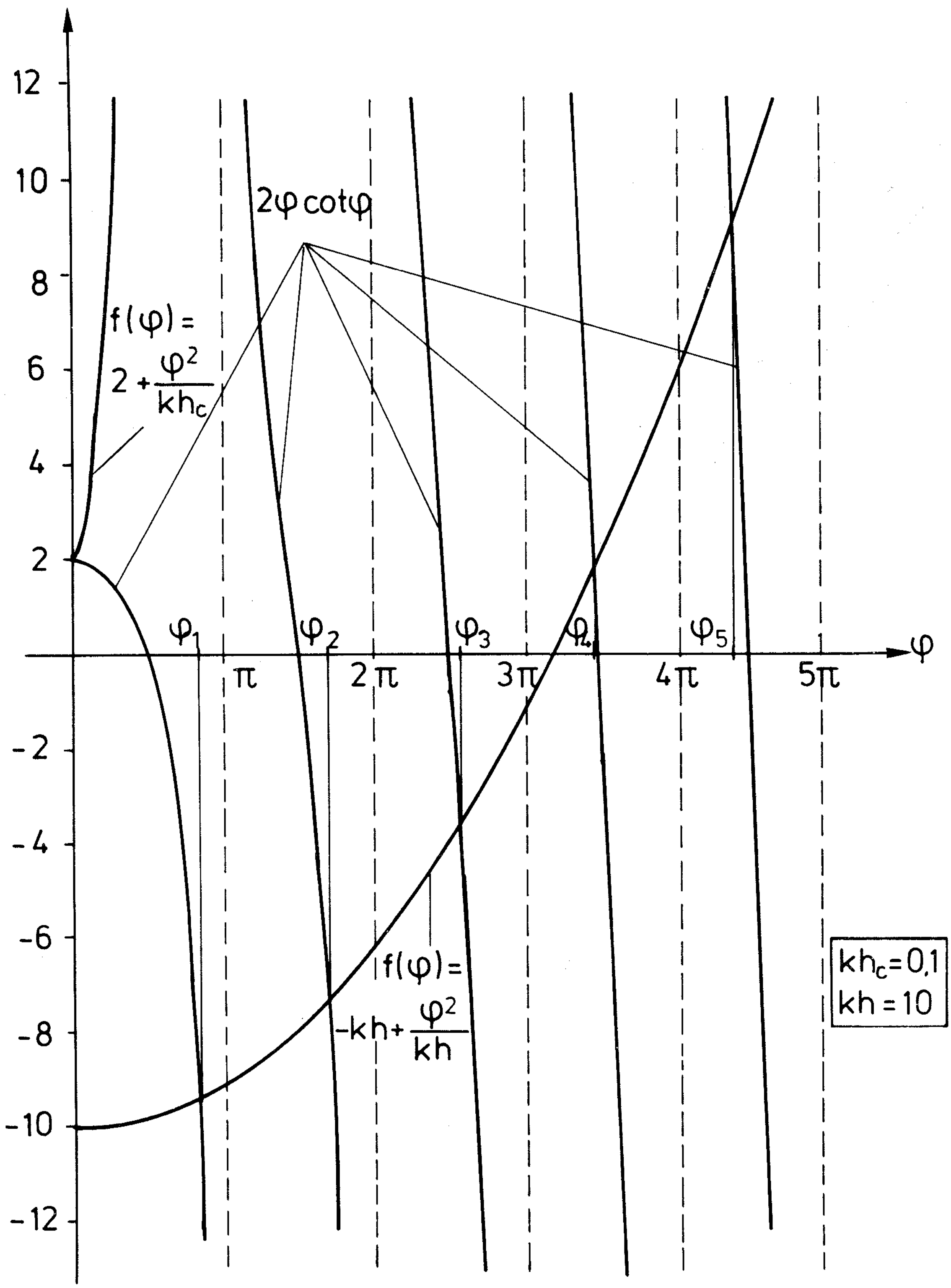

Fig.3: Graphical solution of transcendental equation for the vertical eigenmodes

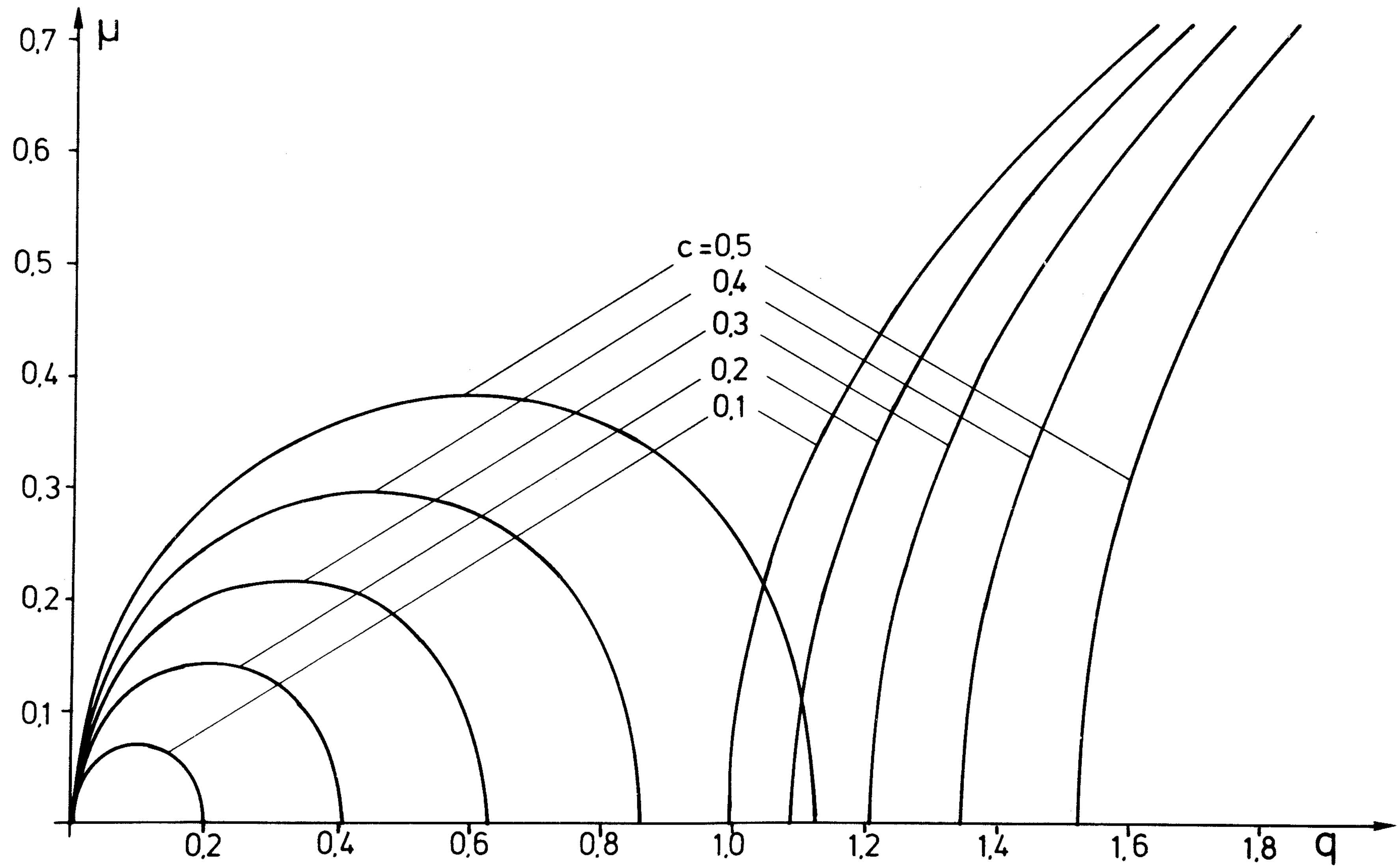

Fig.5: Growth rate μ along straight line $a = -cq$, $c > 0$, $q > 0$, in the instability regions $a < a_o$ and $b_1 < a \ll a_1$ of the Mathieu chart

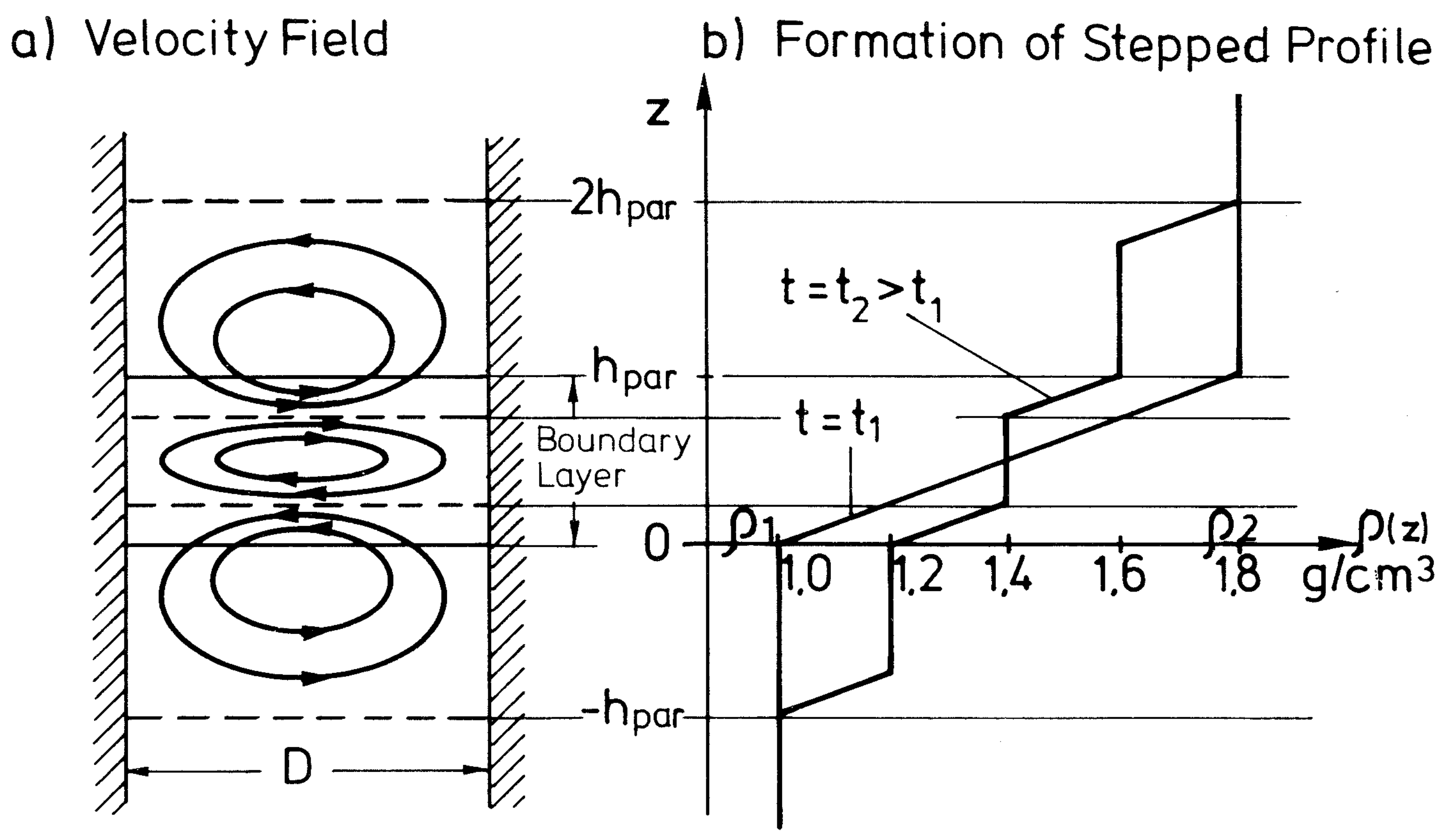

Fig.6: Phase I, formation of stairs

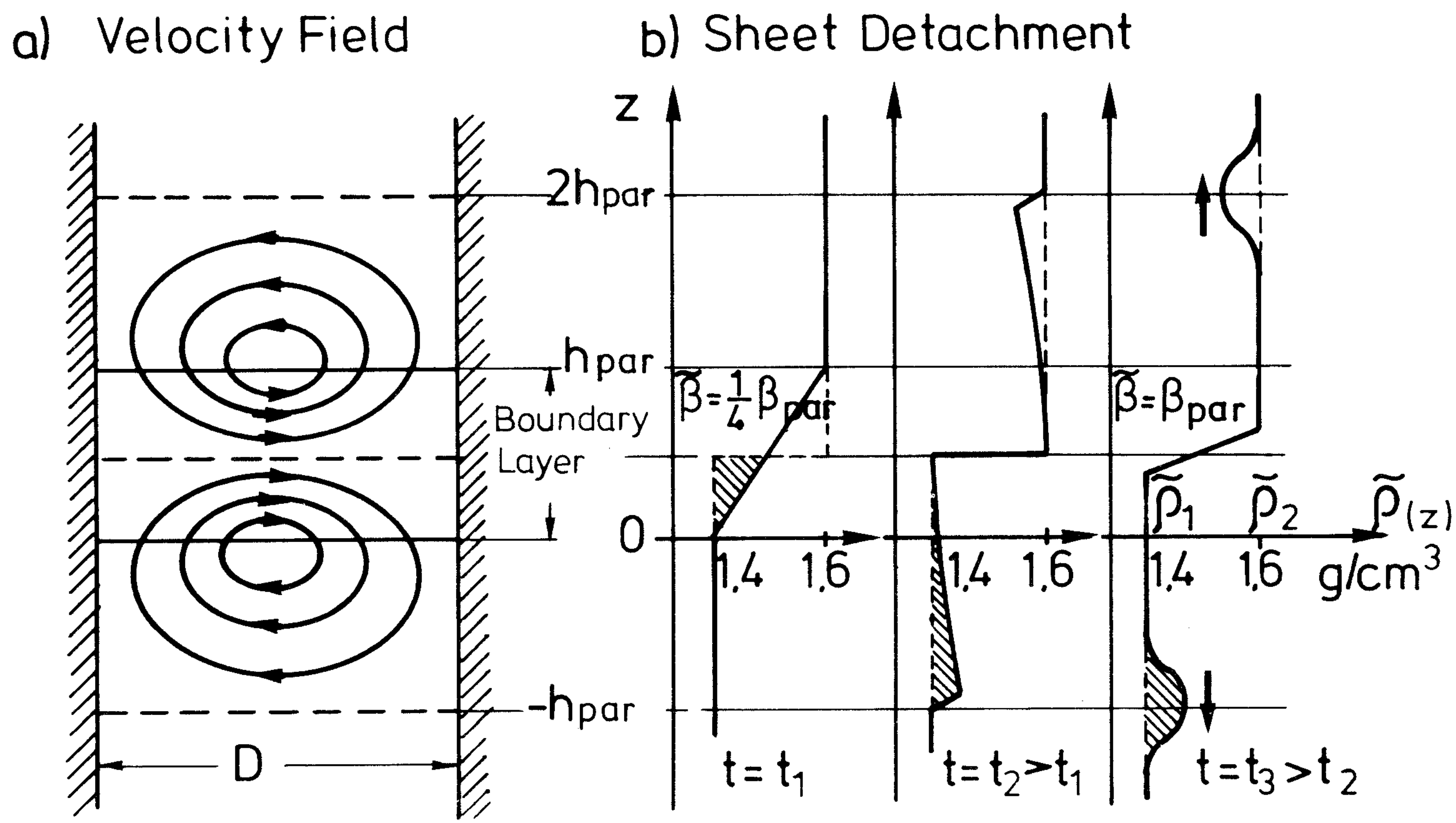

Fig.7: Phase II, periodical sheet detachment

Fig.8: Nonlinearly stabilized potential of vortex motion

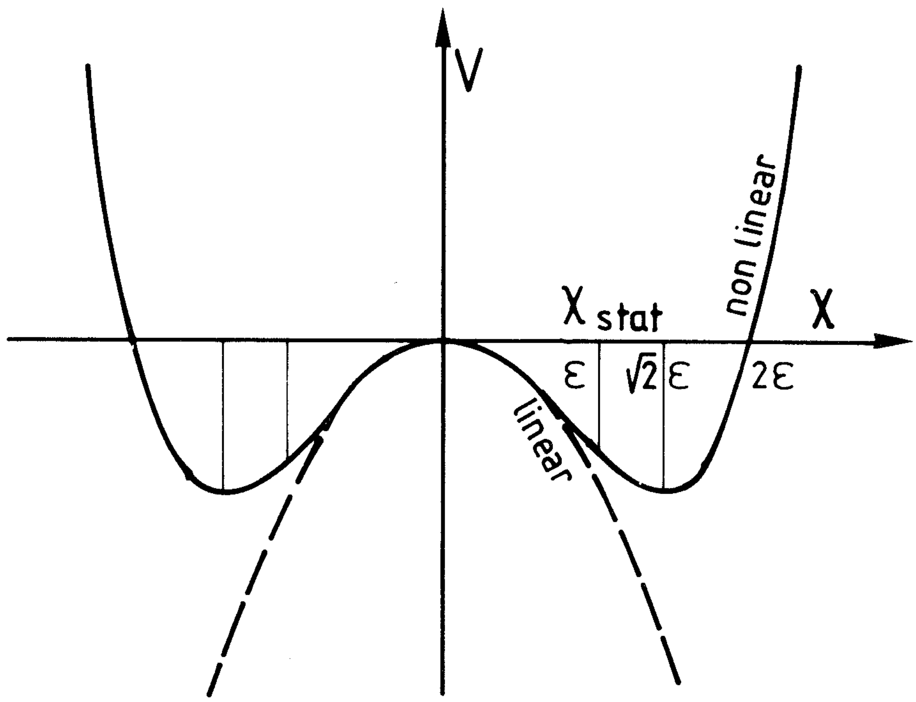

Fig.9: Parametrically limited steepening of density profile